Synthesis of CuS@MSN@SpAcDex for Tacrolimus delivery to treat End Stage Renal Disease

Brajesh Shrestha
39261

Åbo Akademi University

Master´s thesis

Pharmaceutical Sciences Laboratory

Faculty of Science and Engineering

Åbo Akademi University

and

Turku Bioscience Center, University of Turku and Åbo Akademi University

31.03.2021

Master´s degree of Biomedical Imaging
Credits: 45 ECTS

Supervisors:

1: Dr. Hongbo Zhang (Associate Professor)

2: Chang Liu

Examiners:

1: ……..

2: ……..

Passed: ……

Grade: ……

ÅBO AKADEMI UNIVERSITY
Pharmaceutical Sciences Laboratory
Faculty of Science and Engineering
BRAJESH SHRESTHA

Synthesis of CuS@MSN@SpAcDex for Tacrolimus delivery to treat End Stage Renal Disease.

Master´s thesis, 59 pp.
Precision Medicine and Microfluidics
March 2021

Abstract

The treatment of End stage renal disease (ESRD) is kidney transplantation. In order to keep the transplanted kidney safe in the patient's body, it is necessary to kill the patient's immune cells present in the endothelial cells. Although the use of tacrolimus and methylprednisolone drugs was found to be effective in killing patient's immune cells, the traditional oral administration makes these drugs not fully effective because of their poor water solubility and less absorption by the gastrointestinal tract. Thus, an improved therapy such as a drug delivery method is needed, where the complete dose of these drugs, with the help of nanoparticles, will reach the target site and kill the immune cells. Nanoparticles such as MSN and CuS@MSN can load tacrolimus and methylprednisolone, respectively, and deliver them to the target site.

In the present study, the MSN and CuS@MSN were synthesized in the laboratory using an easy and inexpensive method that gives a significant amount of good nanoparticles. The size of MSN and CuS@MSN were ranged from 50-80 nm and 50-120 nm, respectively. In addition, the MSN was loaded with tacrolimus, and the loading efficiency was found to be significantly high (approximately 63%) after the use of MSN and tacrolimus in a 1:5 ratio. In addition, the tacrolimus-loaded MSN was further encapsulated with SpAcDex polymer to form the MSN-tacrolimus-SpAcDex complex for further stability. Furthermore, the zeta potentials of MSN alone and MSN-tacrolimus were measured, and they were -19.1 mV and -19.5 mV.

These MSN and MSN-tacrolimus-SpAcDex were treated with HUVECs for 2 hours, with the help of WST-1 assay, in order to determine the *in vitro* cell viability and cytotoxicity. The WST-1 assay was found to be precise, sensitive, reliable, inexpensive, and fast. The assay showed that both nanoparticles and nanoparticle complexes do not pose any cytotoxicity and do not inhibit the growth of HUVECs. In addition, they are biocompatible. Furthermore, the cellular uptake of these nanoparticle complexes was confirmed after the result of confocal microscopy. Thus, MSN and MSN-tacrolimus-SpAcDex complex can act as a good vehicle for drug delivery methods.

KEYWORDS:

Nanoparticles, MSN, CuS@MSN, SpAcDex, Tacrolimus, Zeta potential, HUVECs, Drug delivery

List of used abbreviations

AcDex	Acetalated Dextran
API	Active Pharmaceutical Ingredient
CFM	Confocal Microscopy
CuS	Copper Sulfide
CuS@MSN	MSN dopped Copper Sulfide
DAPI	4′,6-diamidino-2-phenylindole
DLS	Dynamic Light Scattering
DMSO	Dimethyl Sulfoxide
EC	Endothelial cell
ESRD	End stage renal disease
HUVEC	Human umbilical vein endothelial cell
MSN	Mesoporous Silica Nanoparticle
NM	Nanomaterial
NP	Nanoparticle
PBS	Phosphate-buffered saline
PFA	Paraformaldehyde
SpAcDex	Spermine Acetalated Dextran
TEM	Transmission Electron Tomography

Contents

1. Literature Review 1

1.1 Nanomaterials, Nanoparticles and Nanotechnology 1

1.2 Types of nanomaterials 3

1.3 Mesoporous Silica Nanoparticles (MSN) 6

1.4 MSN dopped Copper Sulfide (CuS@MSN) 8

1.5 Sources and formation of Nanomaterials 10

1.6 Effect of nanoparticles on health and environment 11

1.6.1 Positive effect of nanomaterials 11

1.6.2 Negative effect of nanomaterials 11

1.7 Tacrolimus 12

1.8 Methylprednisolone 13

1.9 Spermine Acetalated Dextran (SpAcDex) 13

1.10 End-stage renal disease (ESRD) and its treatment 15

1.11 Human umbilical vein endothelial cells (HUVECs) and Cytotoxicity measurement 16

1.12 Microfluidics 17

1.12.1 Fabrication of nanomaterials by microfluidics 17

1.12.2 Advantages of microfluidics 18

1.12.3 Microfluidics for Drug Delivery System 20

2. Aim and Hypothesis 21

3. Materials and methods 22

3.1 Materials 22

3.2 Synthesis of MSNs 22

3.3 Synthesis of CuS@MSNs 23

3.4 Preparation of different concentration of tacrolimus solution 24

3.5 Loading of tacrolimus into MSNs 24

3.6 Dynamic Light Scattering (DLS) and Zeta potential 25

3.6.1 Dynamic Light Scattering (DLS) 25

3.6.2 Zeta potential measurement 26

3.7 Microfluidics 28

3.7.1 Design, structure and making of microfluidic chip 28
3.7.2 Setup of microfluidics experiment 30
3.8 In vitro cell viability and cytotoxicity measurement 32
3.9 Imaging 34
3.9.1 Transmission Electron Microscopy 34
3.9.2 Confocal Microscopy 35
4. Results 37
4.1 MSNs under Transmission Electron Microscope (TEM) 37
4.2 CuS@MSNs under Transmission Electron Microscope (TEM) 38
4.3 Loading of Tacrolimus with MSNs 39
4.4 Zeta potential measurement of MSN 41
4.5 Microfluidics 42
4.6 In Vitro Cell Viability and cytotoxicity measurement 42
4.7 Cells under Confocal Microscope (CFM) 43
5. Discussion 46
5.1 Synthesis of MSN and CuS@MSN in the laboratory is easy and the outcome is good 47
5.2 Loading of tacrolimus into MSN is easy, convenient, low cost and has significantly higher efficiency 48
5.3 The value of zeta potential determines the physical stability of MSNs 49
5.4 MSNs and MSN-tacrolimus-SpAcDex complexes do not pose any cytotoxicity to HUVECs 51
6. Conclusion 52
7. Limitation of the study and Future work 53
8. Acknowledgements 54
9. References 55

1. Literature Review

1.1 Nanomaterials, Nanoparticles and Nanotechnology

Nanomaterials (NMs) are defined as materials with any external dimension in the nanoscale or with internal structure or surface structure in the nanoscale range (iso.org, 2021). The term nanoscale represents the scale with the range of 1-1000 nanometer (nm). The nm is an International System of Units (Système international d'unités or SI in French) that represents the length of 10^{-9} meters. To put a nanometer in context, a strand of DNA is about 2.5 nm wide, a red blood cell is about 7,000 nm, and a human hair is about 80,000 nm wide. Thus, the nanomaterial is a broad term, and theoretically, any material having a length of 1-1000 nm in any direction is a nanomaterial. In addition, this is the reason why there is no single internationally accepted definition of nanomaterial does exist, but various definitions in various aspects are used to coin the term nanomaterial (Jeevanandam et al., 2018).

Similarly, nanoparticles (NPs) are materials having a diameter of 1-100 nm in size (Khan et al., 2019). Due to the smaller size of nanoparticles as compared to nanomaterials, it is said that all nanoparticles are nanomaterials, but not all nanomaterials are nanoparticles.

Nanomaterials are considered a bridge between bulk (macro or large scale) materials and atomic or molecular structures. In addition, they are the “first generation” product of nanotechnology and might have 0, 1, 2, or 3 dimensions. Thus, this dimension, along with the shape, is used to term nanoparticles.

A bulk material usually has constant physical properties; however, this might not be true in nanoscale. Nanomaterials usually have unique physical and chemical properties. In addition, these properties are the result of complexity in the atomic and molecular origin. One peculiar fact of nanomaterial is that they can exhibit novel characteristics compared with the counterpart in bulk. The mechanical, electronic, conductive, optical, and chemical properties of these nanomaterials are unlike their bulk ones. Thus, it will be difficult to predict the actual physical and chemical properties of these nanomaterials at the nanoscale. It means that they can show different characteristics in different forms even when they have the same chemical composition. Like nanomaterials, the physical and chemical properties of these nanomaterials are the result of complexity in the atomic and molecular origin.

Some of the nanomaterials are better at heat or electricity conduction, some are chemically more reactive, some reflect much light, and some change color according to

their size (Nanotechnologies, 2020). For example, some nanomaterials possess unexpected visible properties as they are small enough to confine their electrons and produce quantum effects because the quantum effect is dominant on the nanoscale level. For instance, gold appears yellow in the bulk one, however, its nanoparticles appear deep red to black in solution one (ScienceDaily, 2020). In other words, they possess unique physical and chemical properties because of their nanoscale size, along with the high surface area to volume ratio.

At nanoscale level (also in nanoparticles), weak Van der Waals forces but strong polar and electrostatic interaction of covalent interaction exists in the form of particle-particle interaction. This interaction depends upon the viscosity and polarization of the fluid, and it affects the extent of particle aggregation. So, modification of the surface layer charge around the nanoparticle is used to enhance or hinder the nanoparticle aggregation, which ultimately affects the behavior of the nanoparticle (Nanotechnologies, 2020).

As nanoparticles are much smaller than the wavelengths of visible light (400-700 nm), they are unable to be visualized with ordinary light microscopes. Thus, they need electron microscopes for visualization. In addition, these nanoparticles are so minute that they require special nanofiltration filters called ‘Nano filters’ for separation purposes. There are different types of separation methods for nanoparticles, and the criteria behind the selection of separation methods will be determined by the nanoparticle parameters, such as size, shape, and density (Robertson et al., 2016).

Nanotechnology is the study or application of materials at an extremely small level i.e. nanoscale level. It comprises a wide range of physics, chemistry, biology, material science, and engineering fields to deal with at the nanoscale level. The first person who imagined the nanoparticles is an American Physicist Richard Feynman in 1959. He proposed the idea of a possible manipulation or control of individual atoms and molecules. That is why he is known as the father of nanotechnology. However, it is only after the ten years of Richard Feynman's invention, Professor Norio Taniguchithe has coined the term Nanotechnology. Furthermore, it was possible to visualize individual atoms and nanoparticles only after the invention of the Scanning tunneling microscope (STM) in 1981 by IBM researchers.

Nanomaterials have unique and enhanced properties such as higher strength, lighter weight, increased control of light spectrum, and greater chemical reactivity when compared with their larger size counterparts. Some of them are even revolutionary in different fields. Moreover, different types of nanomaterials have different types of specific properties, and these properties enable them to use in wide ranges with various applications such as medicine or drug, transportation, information technology, energy, and food safety. In other words, these nanomaterials are being commercialized.

1.2 Types of nanomaterials

The main parameters for the nanomaterials are their shape (also aspect ratios in some cases), dimension, and their morphological sub-structure. nanomaterials are usually present as an aerosol (solid or liquid phase in the air), a suspension (solids in liquids), or an emulsion (two liquid phases). There are various classification bases of nanomaterials, such as composition, size, and dimension. Here, the nanomaterials can be classified into the following mains, based on their composition.

i. Carbon-based nanomaterials (CBNs)

As the name suggests, the CBN comprises carbon as the main component, and there are different forms of these nanomaterials available. The diverse form of allotropic carbon gives the possibility of unique physical and chemical properties (Cha et al., 2013), and this diversity results in the varieties of morphologies, such as hollow tubes, spheres, and ellipsoids (Sudha et al., 2018). Carbon nanotube (CNT), graphene oxide (GO), graphene quantum dot (GQD), and fullerenes are some of the examples of carbon-based nanomaterials.

CNTs are graphene sheets rolled into a tube, so they have hollow structures. They are good in mechanical strength, electrical conductivity, and optical properties. In addition, their properties, such as higher solubility, biocompatibility, and cellular response, can be altered with the help of their chemical modification. Hence, they are good at various biological applications, for instance, agents for cell and tissue labeling and drug delivery system (Cha et al., 2013). In addition, they are used for structural reinforcement as they are 100 times stronger than steel.

Graphene oxides are oxidized forms of graphite materials and form stable colloids in water due to their hydrophilic nature. They are good at absorbing near-infrared, visible, and ultraviolet light. That is why, they are used as photothermal agents (Kalash et al., 2016).

Fullerenes are allotropes of carbon and have a hollow cage structure (football-shaped) made up of 60 or more carbon atoms. That is why they are denoted by C60. These carbon atoms are arranged in a pentagonal or hexagonal shape. They are used in wide ranges of applications because of their electrical conductivity, structure, high strength, and electron affinity. For instance, they are used as an efficient contrast agent for MRI and X-ray (Lalwani and Sitharaman, 2013).

ii. Inorganic-based nanomaterials

This type of nanomaterials are metal and metal-oxide nanomaterials, so they are made up of metal precursors. Nanomaterials containing iron, gold, silica, silver, or their oxides are examples of such types of nanomaterials. They can be prepared by chemical, electrochemical, or photochemical methods.

They possess good mechanical strength, thermal stability, and optical property. Moreover, having good optical properties, they can be used in biomedical applications such as imaging. For instance, superparamagnetic iron oxides can be used for MRI and gold nanomaterials for acoustic imaging. Besides typical imaging, they are used for stem cell tracking, antimicrobial activity, implant coatings, cross-linkers, and as an agent for drug delivery systems (Zengin et al., 2020).

Ceramic nanoparticles are another example of inorganic-based nanomaterials. They are made up of oxides, carbides, carbonates, and phosphates and are synthesized by heating and successive cooling. Moreover, they exist in different states such as amorphous, polycrystalline, dense, porous, and hollow forms (Sigmund et al., 2006). High heat resistance and chemical inertness are the special characteristics of ceramic nanoparticles. Thus, they are used to protect biomacromolecules from external pH and temperature (Carvalho et al., 2019). Furthermore, imaging applications, drug delivery systems, and dye applications also use these nanoparticles (Thomas et al., 2015).

A common example of ceramic nanoparticles is Mesoporous silica nanoparticles (MSNs), which are inorganic based in nature. One of the interesting features of MSNs is, they can act as a significantly efficient vector during drug delivery systems compared to their organic counterparts (Zengin et al., 2020).

iii. Organic-based nanomaterials

All the nanomaterials made up of organic matter, except the carbon-based ones, fall under the category of organic-based nanomaterials. Organic matters such as lipid-based, protein or peptide-based, and polymer-based nanoparticles are organic-based nanomaterials. Examples of this type of nanomaterials are liposomes, micelles, ferritin, polymers, and dendrimers.

Liposomes contain lipid material as the main component and are round in structure. They have a diameter of 10-1000 nm, and they consist of one or more layers of lipid, which surrounds the aqueous space. They are used for drug delivery (Puri et al., 2009) and RNA release in cancer therapy (Gujrati et al., 2014).

Micelles are spherical in structure and amphiphilic in nature. They consist of a hydrophobic core, but the shell is hydrophilic. They are formed by the supramolecular self-assembly of surfactants and lipids (Euliss et al., 2006 and Enrico, 2018), and their size ranges from 5-100 nm (Oerlemans et al., 2010 and Alexander-Bryant et al., 2013).

Polymers (also known as Polymeric nanoparticles) contain biodegradable polymer, and their shape depends upon the method of their preparation. They can be either nanosphere or nano-capsular shaped (Mansha et al., 2017). Because of having a biodegradable property, polymers are useful for tissue engineering, drug delivery, and new vaccination strategies (Alexander-Bryant et al., 2013).

Dendrimers are highly branched polymers synthetically but behave like micelles. Thus, they show properties of both polymers and micelles, and because of having this property, they can be used for scaffolds for tissue repair, drug delivery, and as a ligand (Virlan et al., 2016).

iv. Composite-based nanomaterials

These are hybrid types of nanomaterials, which contain two or more types of nanomaterials. In addition, each of them should possess unique physical and chemical properties (Luo et al., 2015). Thus, they could be a mixture of any type of nanomaterials. For instance, a mixture of carbon-based and organic-based nanomaterials or a mixture of organic-based and inorganic-based nanomaterials. The good thing about this type of nanomaterial is, it can be tailored, according to the need of applications (Jeevanandam et al., 2018).

There are generally two types of composite-based nanomaterials viz. polymer-based and non-polymer based. These are used in the areas of the development of new functional materials, effective utilization of energy, wastewater treatment, and biochemical medicine (Luo et al., 2015).

v. Semiconductor nanomaterials

Besides these nanomaterials, there is another type of nanomaterial which can show both metallic and non-metallic properties at a different time, and this type of nanomaterials are called semiconductor nanomaterials. In addition, this type of nanomaterials has a much higher linear refractive index compared with the surrounding glass matrix.

The semiconductor has more bandgap than conductors and less than insulators and tuning of this bandgap can result in different types of properties with the same material. In addition, this is the primary reason for using semiconductor nanomaterials to use in

photocatalysis, optical and electronic devices for various biomedical applications (Sun et al., 2000).

Quantum dots (QDs) are examples of semiconductor nanomaterials. They are artificial nanocrystals and can transport electrons. They can glow and emit light of various colors, after the stimulation by an external source, for instance, UV rays. The emitting color varies according to the size and number of the quantum dots. These are very useful in a wide range of applications such as future quantum computers, medical applications, high-resolution screens, solar cells, and fluorescent biological labels (Azonano, 2006.)

As mentioned already, nanomaterials (also Nanoparticles) have wide ranges of application in biomedical, optical, and electronic fields due to their characteristic properties. Among these applications, nanomedicine, along with drug delivery, is one of the interesting characteristics in clinical trial fields. In this field, Nanotechnology helps to provide cheaper but more reliable systems for drug delivery as these nanoparticles can act as carriers for different types of drugs or medicines. During this procedure, materials will be built in the nanoscale (the synthesis of nanoparticles) and used to load the variety of drugs in a slow and controlled way. These drug-loaded nanoparticles are termed vectors or carriers, and a wide variety of nanoparticles are available that can be used as vectors for drug delivery to treat different types of diseases. Among these nanoparticles, Mesoporous Silica Nanoparticles (MSNs) and MSN dopped Copper Sulfide Nanoparticles (CuS@MSNs) will be focused on this study.

1.3 Mesoporous Silica Nanoparticles (MSN)

MSNs are inorganic-based nanomaterials, and as they have a 50-450 nm range of diameter (Karimi et al., 2016), they are usually called nanoparticles instead of nanomaterials. They are primarily made up of silica, and silica has been “Recognized as safe” by the United States Food and Drug Administration (FDA). Structurally, they have a solid framework and are spherical. In addition, they comprise a honeycomb-like porous structure arranged in a 2D network. According to the International Union of Pure and Applied Chemistry (IUPAC) nomenclature, materials whose pore diameter ranges between 2-50 nm are known as mesoporous material (Rouquerol et al., 1994). Hence, these nanoparticles are termed mesoporous silica nanoparticles as they contain silica as the main component, and their pore diameter ranges between 2-50 nm. In addition, these porous structures have hundreds of empty channels and possess a large surface area. A typical structure of an MSN is shown in Figure 1.1. Those large surface areas are enriched with silanol groups. Thus, the availability of such spaces enables them to

absorb or encapsulate bioactive molecules in large amounts and attach or react with different functional groups of various drugs, ligands, polymers, fluorescent agents, etc. (Mendes et al., 2018). In addition, such silanol groups enhance the interaction with the phospholipid bilayers of living cells, along with endocytosis stimulation (Karimi et al., 2016). Furthermore, the attached drugs, situated over the surface of MSN, can be subsequently released in a controlled manner (Douroumis et al., 2012). Besides these, there is a possibility of easy modification of the size of such porous structure and the surface. They consist of a hydrophobic core and a hydrophilic outer surface. The core part will be used for drug loading, while the outer surface part for opsonization blocking and easing movement in the system (Bharti et al., 2015).

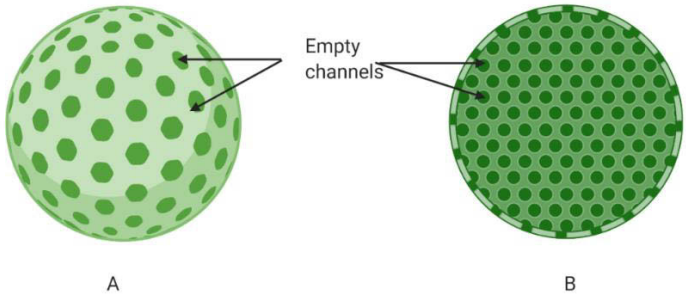

Figure 1.1. A typical structure of an MSN (A = outer view, B = cross section area view). Both views are showing pores like structures, which are actually empty channels.

The typical MSN has three distinct parts, which can be functionalized independently for different purposes. The first part is the silica framework. Usually, imaging agents are attached with this frame to track the MSN for diagnostic purposes. The mesoporous structure, which contains hundreds of pores and empty channels, is the second one. It can be loaded with drugs or any other bioactive molecules. The last part is the outer surface of the particle, and this part can be associated with different types of ligands for targeted delivery. (Karimi et al., 2016).

As MSN contains silica as a basic component, which is widely available in the outer environment compared with other metal or metal-oxides (such as iron, titanium, and gold), it has better biocompatibility than other nanomaterials. The Silica-Oxygen (Si-O) bond is so strong in MSN that it can tolerate external responses and stresses, such as degradation and mechanical stress, compared with liposomes and dendrimers. It makes MSN relatively stable (*in vivo* stability) and biocompatible. In addition, it makes MSN tolerent to several types of chemical modification. In addition, this nanoparticle does not need any external stabilizer during their synthesis (Bharti et al., 2015 and Doan et al., 2018).

The MSN was synthesized by researchers in Japan in 1990 (Tsuneo et al., 1990) for the first time. It is usually synthesized by the condensation of organosilane precursors around organic micelle, with the help of a base-catalyzed sol-gel process. In addition, the honeycomb-like structure mesoporous channels would appear in the silicon oxide matrix by removing the micelle template (Liu and Xu, 2019).

Due to the availability of a large surface area within MSN, each MSN can hold a significant amount of drugs for different purposes. The drug-loaded MSN can be released into the specific tissue or organ, or site with the help of a specific method during the drug delivery procedure. This method helps in the release of any drug concentration directly into the respective site without releasing the drug into the bloodstream, and this process ultimately reduces the side effect of the drug (Li et al., 2012). In this way, MSN could be a good potential vector for the delivery of drugs. The first use of MSNs in the drug delivery system was carried out in 2001 (Vallet-Regi et al., 2001). Here, in this study, MSN will be used to encapsulate the drug tacrolimus.

These MSNs are useful in wide ranges of applications such as drug delivery, diagnosis fields such as imaging, monitoring, biosensors, and thermal energy storage (Valenti et al., 2016).

1.4 MSN dopped Copper Sulfide (CuS@MSN)

MSN alone lacks functional features and might not be fully suitable for the specific function required bio-applications. They also have low biocompatibility as compared to other hybrid nanomaterials. Nevertheless, it can be converted into functionalized one by incorporating different types of inorganic nano-compounds and doing so leads to the development of a wide range of interesting properties in such final nanomaterials (Zhao et al., 2017). In addition, the combination of silica technology with other nanomaterial has provided the possibility of different types of components in a single nanometric entity (Castillo and Vallet-Regí, 2019). One of the examples of such a nanometric entity is MSN dopped Copper Sulfide (CuS@MSN).

CuS nanoparticles are photothermal sensitizer type of nanoparticles, and regarding the photothermal capacity, they are equally good compared to gold nanoparticles. Hence, they are considered as a cheap alternate to gold nanoparticles. They possess a d-d transition of Cu^{2+} ions, which is responsible for the near-infrared (NIR) light irradiation (600 – 1000 nm) and can penetrate through normal tissue without significant thermal injury (Li et al., 2015).

CuS@MSN is a hybrid metal-based inorganic-silica nanoparticle that is composed of a mesoporous silica platform conjugated to copper sulfide (CuS) nanoparticles. It is around 80 nm in size and has high absorption in the near-infrared range with a peak of approximately 980 nm. Thus, the solution of CuS@MSN can convert 980 nm laser to local heat efficiently, and it is the reason why they can be used as a photothermal agent (Chen et al., 2014). The conversion rate is around 56.7%, and this conversion effect is independent of the surrounding environment. This feature is especially useful for photothermal therapy and drug delivery (Li et al., 2015). According to Cai and Chen (2017), it has higher specific surface areas (495 m^2/g) and larger per volume (0.68cm/m3), along with an average pore size of 2.2 nm.

As a typical structure shown in Figure 1.2, CuS acts as the central component and is coated by MSN. The MSN is an external structure and possesses honeycomb-like pores along with empty channels. It is also biocompatible and biodegradable. The MSN will act as both the protective layer for CuS and the reservoir or storage for drugs or bioactive molecules (Chen et al., 2015).

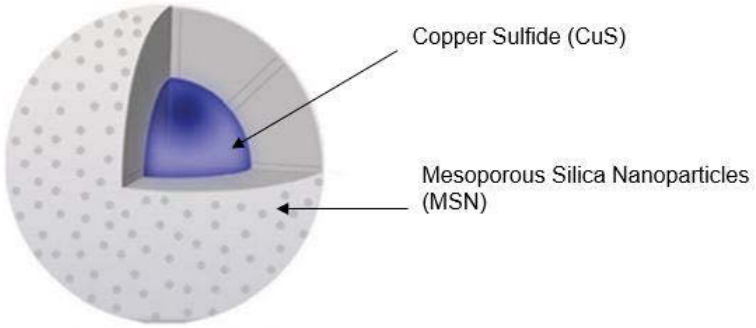

Figure 1.2. A typical structure of CuS@MSN (modified from Peng et. al, 2017). The CuS acts as the core, while the MSN covers the CuS and acts as an external or outer sphere.

These hybrid nanoparticles can be conjugated with other nano-compounds. In addition, they act as both the gatekeepers to prevent the pre-release of drugs and the photothermal agents to kill the target cells (Zhang et al., 2015). This is the primary reason to use CuS@MSN in the drug delivery system.

These nanoparticles are useful in drug delivery systems, bioimaging, and photothermal therapy (Chen et al., 2015). Similarly, they are good to make components of solar cells, electro-conducting electrodes, and different types of sensors, as they are economically efficient (Li et al., 2015).

1.5 Sources and formation of Nanomaterials

Nanomaterials are one of the naturally abundant materials in the world. Besides natural ones, there are also man-made. Therefore, the sources of nanomaterials can be categorized into the following three mains:

i) Nature

Nanomaterials are formed in nature with the help of small or big natural phenomena such as photochemical reactions, volcanic eruptions, forest fires, erosion process, shedding of skins and hairs by living animals. They are produced regardless of human actions and could be released in any spheres of the Earth, such as the atmosphere, hydrosphere, and lithosphere. During the release, some of these nanomaterials are produced in normal and unnoticeable amounts, while some are produced along with other micro-sized particulate matters to such an extent that they will affect the quality of the surrounding ecosystem. For instance, the nanomaterials produced from the photochemical reaction are usually unnoticeable. However, the volcanic eruption produced nanomaterials and other big-sized particulate matters that are not only noticeable but also affect the quality of the surrounding atmosphere (Jeevanandam et al., 2018).

Natural nanomaterials are responsible for 90% of total aerosols present in the air. In addition, these aerosols affect the energy balance of The Earth as they absorb solar radiation and scatter it back to space (Taylor, 2002).

ii) Engineered

Nanomaterials are synthesized in the laboratory in order to acquire peculiar special properties on them for desired applications. It means they are purposely designed and synthesized with the help of physical, chemical, biological, or hybrid methods (Jeevanandam et al., 2018).

Examples of engineered nanomaterials are MSN, CuS@MSN, carbon nanotubes, and quantum dots.

iii) Incidental

Incidental nanomaterials are produced as byproducts during anthropogenic activities, such as cooking, smelting and refining, engine combusting, and chemical manufacturing.

For instance, diesel engine exhaust is an example of incidental nanomaterials. They are similar to the engineered ones. However, the main difference is the control over the morphology of nanoparticles. The morphology of the engineered nanomaterials can be controlled, but the one with the incidental is impossible (Jeevanandam et al., 2018).

1.6 Effect of nanoparticles on health and environment

Humans (also other living organisms) are exposed to trillions of foreign nanomaterial entities every day. In addition, respiration and feeding processes contribute to the entry of a significant amount of nanomaterials inside the body of the living organism. As these nanomaterials are very small in size, it helps them to migrate in the whole biological system easily. In addition, they are much more reactive than their bulk ones, and once they are inside the living body, they could affect the health in either positive or negative ways. Here, both the positive and negative effects are briefly described in the context of humans.

1.6.1 Positive effect of nanomaterials

Nanomaterials such as fullerene derivatives and oxygen vacant compounds (example, CeO_2) could have positive effects on human health. They are antioxidative, neuroprotective, and antiapoptotic, and this nature is responsible for the protection of the liver, kidney, and neuronal cells. Furthermore, nanomaterials derived from silver, titanium dioxide, zinc oxide, and magnesium oxide are known to be antibacterial and especially good against *E. coli* bacteria (Buzea et al., 2007).

1.6.2 Negative effect of nanomaterials

Despite plenty of benefits from nanomaterials, there are some negative effects on human health. The human defense mechanism has never encountered the new genre or engineered type of nanomaterials before, and this type of materials could be very harmful to human health (Jeevanandam et al., 2018). For instance, some nanomaterials are latex sensitive and can cause dermal allergy. Similarly, the antibiotic nature of silver, which is good against bacteria, could be toxic to keratinocytes and fibroblasts. The deposit of a significant amount of nanomaterials can cause Crohn's disease and ulcerative colitis. Besides these, over-exposure of nanomaterials along with other micro materials will lead to cardiovascular malfunction. Another example of health risk is the crossing of the blood-

brain barrier by nanomaterials. If the unwanted nanomaterials succeed to cross the blood-brain barrier, they adversely affect the brain and its surrounding cells (Buzea et al., 2007).

1.7 Tacrolimus

Tacrolimus (also known as FK-506 or Fujimycin) is an immunosuppressive drug that is mainly used after allogeneic organ transplants, such as liver, kidney, heart. It is a calcineurin inhibitor and inhibits T-lymphocyte activity. As a result, it reduces the activity of the patient's immune system that helps to overcome the risk of organ rejection (Ngan, 2004). In addition, it is used for atopic dermatitis, refractory uveitis after bone marrow transplant, and vitiligo.

The molecular formula of tacrolimus is $C_{44}H_{69}NO_{12}$, and Figure 1.3 shows the chemical structure of tacrolimus (DrugBank, 2020).

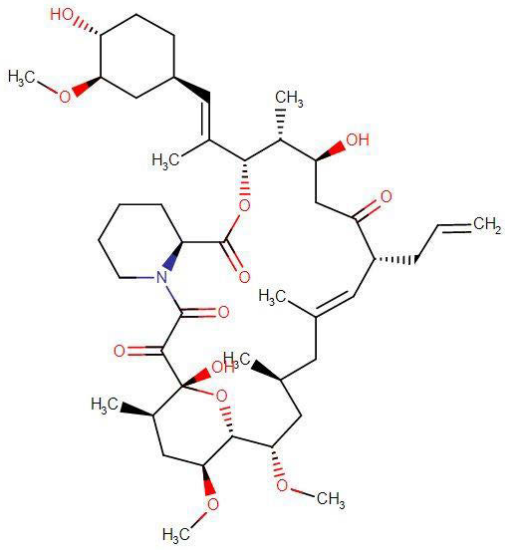

Figure 1.3. Chemical structure of tacrolimus (DrugBank, 2020)

Chemically, it is a macrolide lactone and a lipophilic drug. It is usually available as white or off-white crystals or crystalline powder. In addition, it is soluble in organic solvents such as ethanol and chloroform but insoluble in water. It was first discovered from soil bacteria *Streptomyces tsukubaensis*, present in the Japanese soil sample, in 1984 (RxList, 2018). However, it was only in 1994, when the use of tacrolimus for liver transplantation was approved for the first time by the Food and Drug Administration (FDA). Since then, it was expanded to other organs, such as the kidney, heart, pancreas, lung, and cornea (Pubchem, 2005).

1.8 Methylprednisolone

Methylprednisolone, also known as Medrol, is a corticosteroid drug. It is used to suppress the immune system and treat inflammatory conditions, due to different diseases such as arthritis, ulcerative colitis, and allergic reactions. It is usually white, odorless, crystalline powder, and sparingly soluble in alcohol but insoluble in water (RxList, 2018).

The molecular formula of methylprednisolone is $C_{22}H_{30}O_5$, and the structure is shown in Figure 1.4 (DrugBank, 2020).

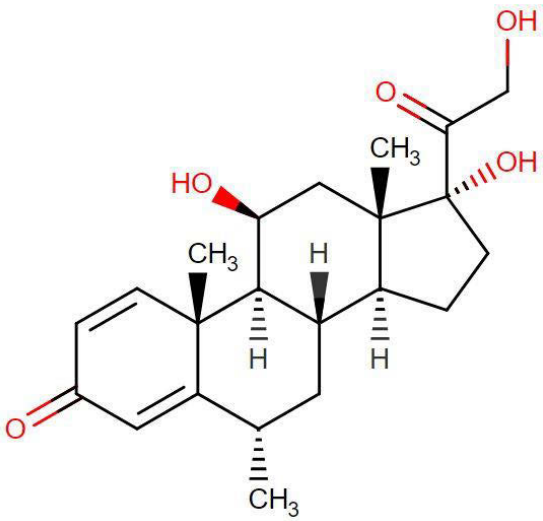

Figure 1.4 Chemical structure of methylprednisolone (DrugBank, 2020)

1.9 Spermine Acetalated Dextran (SpAcDex)

Spermine Acetalated Dextran (SpAcDex) is one of the derivatives of dextran and is commonly used as a polymer to encapsulate various drug or drug-loaded nanoparticles/nanomaterials (e.g., MSN) and cell derivatives (e.g., siRNA). They are easily modifiable and usually the size of 178 - 229 nm. In addition, they are insoluble in water but soluble in organic solvents. (Cohen et al., 2011). Figure 1.5 shows the chemical structure of SpAcDex.

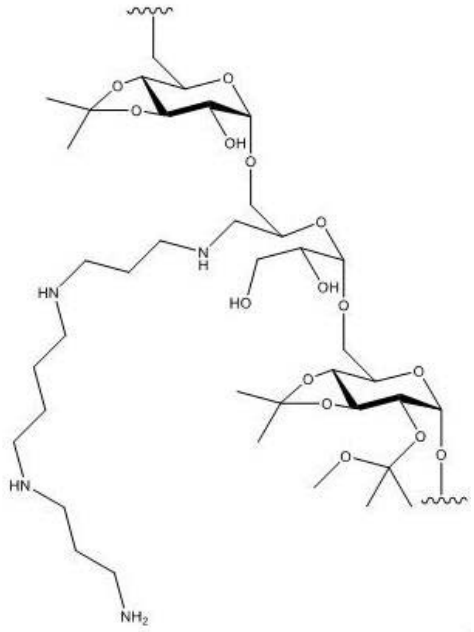

Figure 1.5 Chemical structure of SpAcDex (Cohen et al., 2011)

It is prepared by using reductive amination chemistry for the conjugation of spermine to acetalated dextran (Ac-Dex) (Cohen et al., 2011). The AcDex is a pH-responsive tunable acid-labile dextran derivative biopolymer. In addition, it is used to encapsulate the small molecules and deliver them. (Bachelder et al., 2016 and Wang et al., 2021). Due to its acidic nature, it is useful to deliver the drug into acidic conditions, such as the endosomal chamber, tumor environment, and inflamed area (Wang et al., 2021).

The spermine is attached to the AcDex, and its primary function is to enhance the hydrophilicity, which favors the self-assembly of polymers into nanoparticles. In addition, this feature is often useful for the encapsulation of drugs or nanoparticles.

It is a tetravalent organic amine found in mammalian cells, usually in millimolar concentrations, and at this concentration, it is non-cytotoxic (Mashaghi et al., 2016). However, the non-cytotoxic limitation of SpAcDex is up to 1 mg/ml concentration (Cohen et al., 2011).

It shows high transfection efficiency of plasmid DNA both *in vitro* and *in vivo* and biodegradability features too. It is sensitive to acids. Since it holds a significant amount of positive charge on its surface i.e., cationic in nature, it can form a better complexation with a negatively charged particle. This results in effective targeting into the cell membrane as it can penetrate deeply. It has no cytotoxic effect till 1 mg/ml concentration (Cohen et al., 2011 and Fröhlich, 2012).

Thus, these SpAcDex particles represent cationic polymers and can be used as an effective carrier for drug delivery methods such as carrying siRNA to cancer cells with minimum toxicity (Cohen et al., 2011).

1.10 End-stage renal disease (ESRD) and its treatment

End-stage renal disease / ESRD (also known as end-stage kidney disease / ESKD) is the advanced stage or final stage of kidney disease where the kidney function got lost to such an extent that it no longer can work the way the body needed and therefore need to replace. The only treatment for this disease is kidney transplantation, where a healthy kidney from another person will be transferred into the patient's body (Mayo Clinic, 2020).

However, this kidney transplantation treatment is not as effective as it is supposed to because there is always a chance of antibody-mediated rejections (AMBR). In such a problem, the patient's immune system recognizes the transplanted kidney cells as a foreign agent and tries to kill them. This process is called allograft loss. But the good thing is, several methods can minimize such an allograft loss process. Among them, two methods will be mentioned in this study. The killing of a patient's immune cells, which are responsible for the killing of transplanted kidney cells is the first method. The second method is the inhibition of T-follicular helper (tfh) cells function, along with the inhibition of plasma cell maturation and donor-specific alloantibody (DSA) secretion.

The two methods mentioned above are carried out by using the immunosuppressive drug named tacrolimus. Traditionally, the tacrolimus administration is oral. However, its partial solubility nature with water allows the low absorption via the gastrointestinal tract. Thus, there is a need for an improved therapy that could administer the complete dose of tacrolimus into the target site. For this, a novel approach of drug delivery method, where nanoparticles are carriers, would be a perfect choice. In addition, nanoparticles such as MSN and CuS@MSN can be chosen as carriers.

During this novel approach, the MSNs will be encapsulated with tacrolimus. The encapsulated drug-loaded nanoparticles (MSN-tacrolimus complex) will be further encapsulated with spermine acetylated dextran (SpAcDex) and becomes MSN-tacrolimus-SpAcDex complex. This MSN-tacrolimus-SpAcDex complex will be delivered to tfh cells via a specific type of ligand (here CD40L). During targeting, the encapsulated drug will be modified with a specific antibody (here CD40LAb) to target tfh cells. This combined drug and nanoparticles along with antibodies impair the plasmablast formation and DSA secretion and finally leads to the inhibition of DSA production. Furthermore, it reduces the tfh's functions.

The biomarker of ABMR is a complement compound (C4d). There is no presence of C4d in own kidney cells but present in the transplanted kidney. In addition, the primary function of C4d is to activate the host's immune systems and thus activated immune system ultimately kills the transplanted kidney cells as it is recognized as a foreign agent.

To mitigate this problem, the methylprednisolone drug will be loaded into CuS@MSNs and encapsulated with SpAcDex polymer to form CuS-MSN-methylprednisolone-SpAcDex complex. These nanoparticle complexes will target the immune cells, where they produce heat by local inflammation, and this heat kills the immune cells.

1.11 Human umbilical vein endothelial cells (HUVECs) and Cytotoxicity measurement

HUVECs are one of the types of endothelial cells (EC) that are isolated from the umbilical vein of the umbilical cord, and this umbilical cord is normally get resected after childbirth. The umbilical cord connects the fetus to the mother's blood supply through the placenta during fetal development. In addition, the umbilical vein carries the blood to the fetus while the umbilical arteries carry away the blood from the fetus. These blood supplies deliver oxygen and nutrients to the fetus to grow and survive (Lifeline Cell Tech Team, 2020).

HUVECs are used as a laboratory model system to study the function and pathology of the endothelial cells, for instance, angiogenesis. They are inexpensive, and the technique used to isolate contamination-free HUVECs, from the umbilical cord is not complicated. They are easily available because they are considered biological waste after childbirth. Since HUVECs are the most studied and available type of vascular endothelial cells, they are used for a wide range of experiments, such as vascularization of various engineered tissues and toxicity measurements. The first isolation of HUVECs, along with their *in vitro* culture, was carried out by Jaffe and others in 1970 (Kocherova et al., 2019).

The nanoparticles prepared in this study are supposed to be in direct contact with the normal endothelial cells of the kidney. That is why these nanoparticles need to be tested for toxicity against the endothelial cells that cover the lumen of blood vessels. This will make it easy to understand if any probable adverse effect of these nanoparticles with relevant cells. Therefore, to execute such an experiment, HUVECs *in vitro* model will be the best one, among others. This model will help to explore the nanoparticle - endothelial cells (NP-EC) interactions and the toxic effect of nanoparticles on endothelial cells. Furthermore, it is considered a relatively reliable and simple *in vitro* model for ECs to predict and evaluate the toxicity of nanoparticles to the endothelium (Cao et al., 2017).

Here, in this study also, HUVECs will be used as a replacement of normal endothelial kidney cells because both cells resemble each other too much extent. Besides this, HUVECs are easily available and are easy to experiment with compared to normal

endothelial kidney cells. In addition, their proliferation rate can fluctuate with laboratory settings. Furthermore, their experiment can be performed at normal laboratory temperatures.

1.12 Microfluidics

Microfluidics is the branch of science that is used to study fluid systems, which can process small quantities of fluids (10^{-9} - 10^{-18} Liter) by using tiny channels having microscale dimensions, usually tens to hundreds of micrometers. It is a non-turbulent system and is made up of highly miniatured devices that contain networks of microchannels for fluids to pass through or be contained in. (Mousavi et al., 2019). Thus, it can manipulate small volumes of fluid (up to femtoliters) in a precise manner and the behavior of this amount of fluid, which is often quite different than their macroscale in everyday life, can be monitored. This character enables the microfluidic system to synthesize both the biological and the non-biological particles up to the nanosized range. In addition to the synthesis process, it can increase or decrease the transfer rate of ingredients, which ultimately affects the rate of chemical reactions. This feature is essential for sensing mechanisms which require a binding reaction at a solid surface, such as in DNA and protein chips (Stroock, 2008).

It is one of the novel and breakthrough technologies. Despite its position in a nascent stage, it is rapidly emerging and has a big potential for several applications in different fields, such as biology, chemistry, information technology, and optics.

1.12.1 Fabrication of nanomaterials by microfluidics

Microfluidics can fabricate several types of nanomaterials as it can control different types of parameters. Some of them are as follows:

i) Inorganic and hybrid nanoparticles

Inorganic and hybrid nanoparticles can be fabricated with the help of microfluidics. Inorganic materials, such as metals and their oxides and silica, are used for this process. Examples of such nanoparticles are MSN and CuS@MSN.

ii) Lipid-based nanoparticles

Lipid-based nanoparticles such as liposomes and lipid nanoparticles (LNPs) can be synthesized through microfluidics. These nanoparticles are biocompatible and good at loading of drugs.

iii) Polymer-based nanoparticles

These types of nanoparticles are synthesized by the emulsion cross-linking process, and the solvent is either evaporated or replaced with the non-solvent. Poly-Lactic-co-Glycolic Acid (PLGA) is an example of polymer-based nanoparticles.

iv) Protein- or biomembrane-based nanoparticles

Protein- or biomembrane-based nanoparticles, such as HDL- mimicking nanomaterials (μHDL), are another example of nanoparticles that could be fabricated by microfluidics. These are good for drug loading to target tumors.

v) Lipid −Polymer Hybrid Nanoparticles

These types of nanoparticles are fabricated by combining two or more types of nanoparticles, and as a result of having multiple nanoparticles together, they provide multiple benefits.

vi) Lipid −Polymer Hybrid Nanoparticles

Another type of nanomaterial, such as pharmaceutical nanomaterial, can be synthesized with the help of microfluidics. An example of this type of nanomaterial is the pharmaceutical colloidal sphere. (Zhang et al., 2019).

1.12.2 Advantages of microfluidics

As fluids act differently on a micrometric scale than the macroscale ones in everyday life, this strange feature is used for scientific experiments and innovations. In addition to this, it has the following advantages:

i) High level of precision

Microfluidics system offers heterogeneous systems that are characterized with a high level of precision because of their high-level design and architecture. It is said that even a single cell or molecule in *in vitro* can be manipulated experimentally with the help of microfluidics. The control of parameters is precise too. Hence, the experiment becomes a high-level and precise one. The extreme sensitivity of microfluidics is due to the lower level of detection limits. Thus, it can give high-throughput and highly accurate results in biological or chemical assays (Thomas, 2019).

ii) Time saving

A microfluidic system can run or process several analytes at the same time or simultaneously. This is possible because of the compact size of the analytes they use. The simultaneous running of several analytes ultimately reduces the time to experiment. Furthermore, both the reactants mixing time and the reaction time for the microfluidic system are too short compared to the conventional one. So, the compact size causes reduction of both space and time. Likewise, multi-staged experiments can be executed with the help of microfluidics in a short time. Thus, microfluidics makes the process more efficient and gives more throughput in a short time. (Mousavi et al., 2019).

iii) Cost saving

The reagents and samples used in the biological and chemical assays are often expensive. Furthermore, experimenting at a macroscale level using these reagents and samples would increase the total cost of the experiment. However, the use of microfluidics saves the total cost as it uses a microlevel amount of reagents and samples because of its compact size. Despite the use of a significantly less amount of reagents and samples, the results are very accurate.

In addition, microfluidics systems are highly automated and require minor operator handling. Although there is substantial parameter control over the experiment, the performance of the system can be well-preserved. So, multi-stage experiments can be executed with the help of a microfluidic system even with less expertise. (Mousavi et al., 2019). Furthermore, microfluidics would be the ideal one in a situation, where reagents and samples are very limited, but time-to-result is critical and no professionals are available (Lion et al., 2004).

iv) Accurate result

Microfluidic systems carry out experiments with a microlevel amount of reagents in a short time. It increases both the speed and the accuracy of reactions. Although the experiment time is short, it gives results with higher sensitivity because of the few errors, which arise in a short time compared to the conventional system that takes a long time to experiment. Similarly, as they can execute the experiment well with minor sample handling, the data quality would be excellent. Thus, the results obtained from the microfluidics assays will be highly accurate and trustworthy. (Mousavi et al., 2019).

v) Flexible application

Being compact in the size, even with all their units, microfluidic systems are portable. They can be easily transported, which increases the number of applications they can be used for. Similarly, they can be used in the point-of-care application. (Mousavi et al., 2019).

1.12.3 Microfluidics for Drug Delivery System

There are several delivery methods, such as oral, sublingual, rectal, intravenous, subcutaneous, and intramuscular, and all these delivery methods are available in traditional or conventional drug delivery systems. However, those methods also have plenty of drawbacks, such as low solubility and permeability, the possibility of degradation by various enzymes, interaction with foods, toxicity because of incorrect dose, inflammation, irregular absorption of the drug, and the need to use a large drug-volume. The low solubility and permeability features of hydrophobic drugs disable their complete absorption of the drugs by the gastrointestinal tract (Andrade et al., 2017). Apart from these, there is the possibility of change in the release profile of the drug due to the generation of polydisperse particles, limitation in the generation of carriers for drug loading, and difficulty in the localization of drug in target site (Damiati et al., 2018).

Similarly, during the fabrication of nanoparticles by the conventional top-down method, mechanical stirring or sonication is used to mix an aqueous phased-API and an organic phased-surfactant with a polymer. Thus, this process causes low and uneven API encapsulation and consistency and ultimately low yielding of desirable drugs. (Gray & Abdulkin, 2018).

However, these drawbacks can be overcome by using microfluidics as it provides control over various parameters during the fabrication of nanoparticles and the drug delivery system. It allows control of nanoparticle parameters, such as size, shape, structure, surface engineering, and elasticity during the fabrication of nanoparticles, and gives the possibility to synthesize or fabricate a desirable range of nanoparticles. (Tomeh and Zhao, 2020). As the nanoparticles fabricated by the microfluidics systems are uniform in size and morphology, these are highly stable, they can load more drugs, and they allow slow release of the drugs at the target site (Damiati et al., 2018). In addition, there will be no waste of APIs as they will give almost 100% encapsulation efficiency compared to the conventional one (30%). Furthermore, the polymer encapsulation of hydrophobic drugs does not cause the problem of low absorption by the gastrointestinal tract as these drugs will be directly delivered to the target site (Gray & Abdulkin, 2018).

2. Aim and Hypothesis

The purpose of the thesis study is the synthesis of two different types of nanoparticles with the help of the easiest but the most convenient method. In addition, loading of drugs and encapsulating them with the polymers will be executed. Thus, the main aim of the study can be summarized as follows:

- Synthesis of both solo type of nanoparticles (MSN) and the hybrid type of nanoparticles (CuS@MSN) in a laboratory for research purposes.
- Loading of tacrolimus drug with MSN and calculation of drug loading efficiency by MSN.
- Encapsulation of tacrolimus loaded MSN with SpAcDex polymer to make MSN-tacrolimus-SpAcDex complex for good stability.
- Execute the HUVECs model experiment with the help of proliferation-based cell assay to measure the cytotoxicity of MSN.

This study hypothesizes that the laboratory synthesized MSNs can be efficiently loaded with tacrolimus and further encapsulated with SpAcDex polymer. In addition, these MSNs and MSN-tacrolimus-SpAcDex complexes do not pose any cytotoxicity with endothelial cells of the kidney.

3. Materials and methods

3.1 Materials

Triethanolamine (TEA), 3-Aminopropyl triethoxysilane (APS), Ammonium nitrate (NH_4NO_3), and Cyclohexane were purchased from Acros organics while Cetyltrimethylammonium chloride solution (CTAC, 25 wt %), sodium sulfide nonahydrate ($Na_2S_3.9H_2O$), methanol, and sodium citrate dehydrate were from Sigma-Aldrich (St. Louis, MO). Similarly, Tetraethyl orthosilicate (TEOS), Copper(II) chloride (CuCl2) from Merck, Acetone from Honeywell, Absolute ethanol (99.5%) from Etax, sodium chloride (NaCl) were ordered from J.T. Baker. In addition, Phosphate-buffered saline (PBS) and Paraformaldehyde (PFA) were ordered from BioWhittaker, Lonza.

After purchasing, there was not any further purification of all these chemicals carried out in the laboratory.

3.2 Synthesis of MSNs

There are several methods/protocols available for the preparation of MSNs. Among them, the Sol-Gel method was chosen as a method for the synthesis of MSN. In addition, within the sol-gel method, the protocol from Shen et al. (2014) was followed as it was found to be one of the easiest but the most inexpensive ones, and it gives good quality of MSNs. In addition, the reagents that will be used in the synthesis are easily available.

First, a 100 ml Round-bottom flask (RBF) containing 36 ml of milliQ water was taken. In this RBF, 24 ml (25 wt%) of CTAC solution and 0.18 gm (247 µl) of TEA were added, and it became the water-CTAC-TEA solution. This whole mixture was stirred gently at 60^0C for 1 hour. After 1 hour, 20 ml (10% v/v%) of TEOS in cyclohexane was added to the above water-CTAC-TEA solution. This mixture was left for stirring @ 150 rpm and at 60^0C for the whole night.

On the next day, the mixture was transferred into centrifuge tubes to centrifuge it. The centrifuge process was executed @ 15,000 rpm for 6 minutes, with the help of a centrifuge instrument (Sorvall Lynx 4000 Centrifuge, Thermo Scientific). After centrifugation, the obtained extract was washed with absolute ethanol. This process was repeated at least two times. The thus obtained extract might contain unnecessary templates and to remove these templates, the extract was treated with 0.6 wt% of NH_4NO_3 ethanol solution at 60^0C for 6 hours.

After all these steps, MSN, as the final product, was obtained. It was collected with the help of absolute ethanol and stored in a refrigerator at 4^0 C for experiments.

3.3 Synthesis of CuS@MSNs

During the laboratory synthesis of CuS@MSNs, the protocol from Chen et al. (2015) was followed as it was an easy and inexpensive method, among several methods of CuS@MSN synthesis in the laboratory. The whole synthesis method took place in two phases. The first phase was the synthesis of sodium citrate capped CuS nanoparticles, while the second one was CTAC capped CuS nanoparticles. The schematic diagram of the synthesis of this nanoparticle is shown in Figure 3.1.

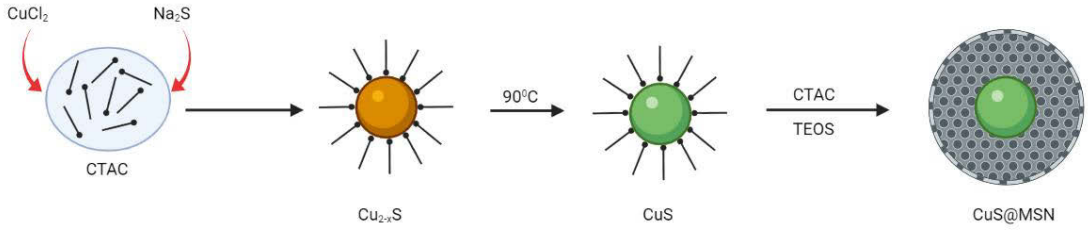

Figure 3.1 Schematic diagram of CuS@MSN synthesis [modified from Lu et al. (2015)]

In the first phase, a 100 ml capacity of RBF was taken, and 30 ml of milliQ water was added to it. In addition, 10 ml of $CuCl_2$ water solution (0.85 mg/ml concentration) ($CuCl_2$ is soluble in water) and 10 ml of sodium citrate (1 mg/ml concentration) were further added. The whole mixture was stirred for about 30 minutes at room temperature with the help of the stirring magnet. After 30 min, 50 µl of Na_2S (60.54 mg/250 ml concentration) was added to the stirring solution, and it was left to stir for 5 minutes. Then, the whole solution was transferred to a water bath of 90^0C temperature for about 15 min. After 15 min, the solution from the water bath was taken out and made cold immediately with the help of an icebox. The cooling down of the solution resulted in the formation of green-colored sodium citrate capped CuS nanoparticles in the RBF. Thus, the mixture or solution present inside the RBF turned into CuS-CTAC water solution.

In the second phase, the solution containing sodium citrate capped CuS nanoparticles, synthesized during the first phase, was used. 20 ml of freshly prepared CuS-CTAC water solution was poured in an RBF, and further 20 mg TEA and 2 gm CTAC (2 wt % solution) was added to the solution. The mixture was stirred for about 1 hour at room temperature. After 1 hour, a total of 200 µl @ 40 µl/min was added to the stirring mixture with the help of an automatic pump, and it was left to stir for another hour. The whole process was conducted in the water bath at 90^0C. When the mixture got cold, it was centrifuged in a

centrifuge machine (Sorvall Lynx 4000 Centrifuge, Thermo Scientific) @ 15,000 rpm for 6 minutes, and the extract was washed with milliQ water to remove residual reagents. The thus obtained product was treated with 1 wt% NaCl solution in absolute ethanol for 24 hours, which helped to remove template CTAC. This treating process was repeated 3 times so that all CTAC templates would be removed. After treatment, CuS@MSNs were obtained as a final product. The final product was stored in a refrigerator at 4^0C for experiments.

3.4 Preparation of different concentration of tacrolimus solution

In order to load the tacrolimus in the laboratory synthesized MSN, the powder form of tacrolimus drug was converted into the solution one. The first solution made from the powder was 100 mg/ml of concentration, which was considered a standard solution for further dilution and experiments. This standard solution is also known as the stokes solution. In addition, the stokes solution was further diluted into different concentration solutions, such as 10 mg/ml, 0.7 mg/ml, 0.6 mg/ml, 0.5 mg/ml, 0.4 mg/ml. 0.3 mg/ml, 0.2 mg/ml, 0.1 mg/ml, and 0.05 mg/ml concentration.

After making the different concentrations of tacrolimus solution, the Ultraviolet (UV) ray intensity of these solutions was measured with the help of the Nanodrop method (Nano drop 2000C Sphectrophotometer, Thermo Scientific). Each measurement and the whole procedure were repeated 3 times, in order to get concurrent data. The nanodrop method helps to quantify the particles present in the solution. Thus, it will be easy to determine the actual concentration strength of tacrolimus in our prepared solution.

3.5 Loading of tacrolimus into MSNs

For this study, the equal concentration of both the tacrolimus solution and the MSN solution was chosen, and hence it was 0.5 mg/ml. The main reason for selecting this concentration was the availability of a significant number of nanoparticles and drug particles in such a concentration. Such a significant number of both particles are essential to carry out the experiments in a proper way. If the number of particles is fewer, no reactions can take place in the way that it is supposed to.

In order to load the tacrolimus into MSNs, both solutions were mixed in different ratios such as 0.5:1, 1:1, 2:1, 3:1, 4:1, 5:1, and 6:1 (Tacrolimus:MSN). The mixture was stirred @ 300 rpm for 24 hours at room temperature. This mixing procedure was done in two sets. The first set of mixture went through centrifugation while the second one did not.

The centrifuge machine involved in this process was from miniSpin, Eppendorf. After mixing both solutions, UV ray absorbance measurement was conducted at 202 nm wavelength with the help of the nanodrop method (Nanodrop 2000C Sphectrophotometer), for both sets. Finally, these data were used to calculate the efficiency of tacrolimus loading in MSN.

As the tacrolimus is loaded with MSN only after the preparation of MSN, the method of loading (absorption) is known as post-sorption. During absorption, tacrolimus is absorbed through the pores and remains in empty channels of MSN. In addition, this absorption process is enhanced by the surface Si-OH groups of the silica by providing two to four linking sites per nm (Karimi et al., 2016).

3.6 Dynamic Light Scattering (DLS) and Zeta potential

3.6.1 Dynamic Light Scattering (DLS)

Dynamic light scattering (DLS) or photon correlation spectroscopy (PCS) or quasi-elastic light scattering (QELS) is a ubiquitous, non-invasive, and well-established method for the measurement of size, size distribution, and surface charge of the particles, typically in the submicron region (Malm and Corbett, 2019). It determines the hydrodynamic size of the particle with the help of both the light scattering mechanism and the analysis of intensity modulation of the scattered light as a function of time (Lim et al., 2013).

3.6.1.1 Principle of DLS

As mentioned above, DLS uses the light scattering method to determine the hydrodynamic size and the nature of their charge present over the surface. The nanoparticles exist in a colloidal dispersion state, where they exhibit Brownian motion. This Brownian motion causes the scattering of light at different intensities. Analysis of these fluctuated intensities determines the hydrodynamic size of the nanoparticles. Similarly, colloidal dispersion is the state of interaction between ions and molecules. This interaction results in the generation of surface charge over them. The nature of these charges will be figured out by the same light scattering method. (LS instruments, 2020).

The analysis of fluctuating light intensities due to Brownian motion is used to calculate the diffusion coefficient as in the following Stokes-Einstein equation.

$$D_t = \frac{k_B T}{6\pi\eta R_H}$$

Here, D_t is the diffusion coefficient, k_B is the Boltzmann constant (1.380649×10^{-23} joule per kelvin), T is the temperature (in kelvin unit) of the colloidal dispersion, η is the viscosity of the colloidal dispersion, and R_H is the radius of the nanoparticles.

3.6.2 Zeta potential measurement

Zeta potential determination is one of the significant characterization techniques of nanoparticles to estimate the nature and value of surface charge (Joseph and Singhvi, 2019). It will help to understand the physical stability of the nanoparticles. Thus, it can be defined as the potential difference between the mobile dispersion medium and the stationary layer of the dispersion medium attached to the dispersed particles. It is used to quantify the magnitude of the charge. Although zeta potential is a charge between two layers, it is not as same as or equal to the Stern potential or electric surface potential between two layers. These are two different types of charges found at two different locations.

Several factors are supposed to affect the nature and amount of the zeta potential, and some examples are the pH of the medium, ionic strength, concentration of the reagents, and temperature. Among them, the pH of the medium is the most significant. However, it is not only the zeta potential that determines the physical stability of the nanoparticles. The presence of surfactants, the property of materials, and the nature of the solution also affect the physical stability of the nanoparticles (Lu et al., 2010).

The value of zeta potential could be either high or low and positive or negative, depends upon the nature of nanoparticles or emulsions. Nanoparticles with high (positive or negative) zeta potential value lead to the better physical stability of nanoparticles because of the electrostatic repulsion of individual particles. The greater the electrostatic repulsion force, it overcomes the total attractive forces, and this total attractive force ultimately makes the nanoparticles physically stable. On the other side, low zeta potential values (either negative or positive) indicate the bad physical stability of nanoparticles. This is because of the aggregation and flocculation of nanoparticles with each other due to Van der Waal's attractive forces acting on them. Generally, zeta potential value ranges from -100 mV to +100 mV. In addition, the zeta potential value within the range of -10 mV to +10 mV is considered neutral. Similarly, the value ranges from -30 mV to +30 mV is considered good because nanoparticles become physically stable at this range, while more than this range is considered excellent because nanoparticles become super stable at this range (Joseph and Singhvi, 2019). Thus, with the help of zeta potential, it will be easy to know how stable the nanoparticles are.

In the present study, the DLS method was conducted for both the MSN alone and the tacrolimus loaded MSN (MSN-tacrolimus). For MSN alone, two different solutions having different concentrations were used. The first one was 0.5 mg/ml concentration while the second one 0.25 mg/ml. The main reason for using these different concentrations was to find out any differences in zeta potential value caused by the concentration strength. Similarly, tacrolimus loaded MSN (MSN-tacrolimus) in the ratio of 5:1 (Tacrolimus:MSN) was used to measure the zeta potential. The general process for the DLS method is shown in Figure 3.2.

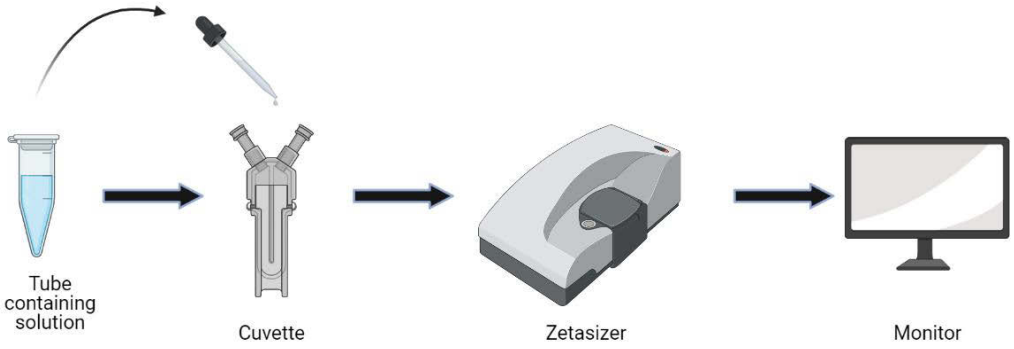

Figure 3.2 Typical steps to carry out the DLS method

In order to carry out the DLS experiment, the solution was poured into a cuvette, and the cuvette was inserted into the DLS machine (Zetasizer, Malvern). After initiating the measurement procedure by the machine, the result was displayed on the screen, and it was noted. The measurement procedure of each solution was repeated two times in order to get the concurrent result. Figure 3.3 shows the machine used for the DLS experiment.

Figure 3.3 Zetasizer machine used for the measurement of zeta potential (Zetasizer, Malvaren)

3.7 Microfluidics

Here, in the present study, tacrolimus-loaded MSN was encapsulated with SpAcDex polymer with the help of microfluidics system (PMD, Harvard Apparatus). For this, a device was used, which is a basic pump for pumping the liquid. In this experiment, two such pumps were used at the same time. Besides these, a microfluidic chip was also used, where mixing and encapsulation of MSN-tacrolimus and SpAcDex took place in a planned manner.

3.7.1 Design, structure and making of microfluidic chip

There are several types of microfluidic chips available in the market for different purposes. However, the one used for this study was self-designed and made in the laboratory, and the theory behind the chip design was from the protocol of Chen et al., 2015. The chip was designed as a T-junction type. It is called the T-junction type as it looks like the letter 'T', and because of this, it has a simple geometry. It forms the passive droplet with the help of hydrodynamic or gravitational forces. Thus, it is easy to manipulate, operate and control. In addition to these, it creates a relatively high monodisperse type of droplets at a higher rate consistently (Lu, 2018). Another benefit of using a T-junction type of chip is, there will be a lower variation of droplet size during the experiment, and the formation of droplets will continue even at less favorable conditions (Ushikubo et al., 2014). The chip might have one or more 'T' junctions, and for this study, two 'T'-junction type was designed and made. Figure 3.4 shows the schematic design of the chip used in the experiment.

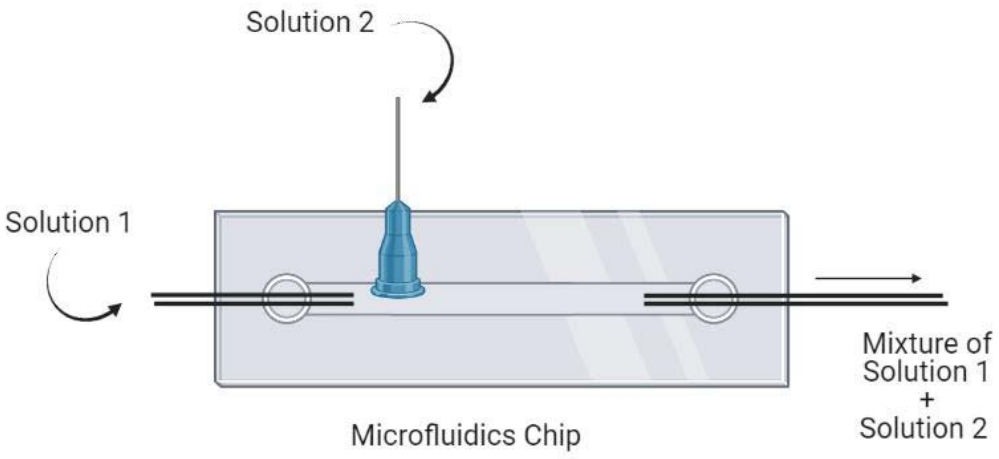

Figure 3.4. Schematic design of the microfluidic chip used in the experiment.

The T-junction type of microfluidic chip was made, according to the design from Figure 3.4. The required components for this process were a regular microscope glass slide (Thermo Scientific), two different types of borosilicate glass tubes, each having two different internal diameters (0.58 mm and 1.56 mm), syringe caps, and needles. Here, the glass tube with a bigger diameter will be said the outer tube while the smaller ones, the inner tube. Apart from these, a needle puller (PN-31 Magnetic Glass Microelectrode Horizontal Needle Puller, Narishige Japan) to cut out glass tubes, and Epoxy resin, along with hardener, for sticking purposes were also needed. The first step was cutting glass tubes with the help of a puller so that each glass will be symmetrical and has cone shape endings. The cone-shaped end of each glasses was treated with sandpaper so that each of them will have smooth edges along with symmetrical openings. These openings needed to be symmetrical because it is the place where all mixing of solutions/reagents will take place during the experiment.

The outer tube was cut with a diamond cutter and put in a specific place that will be covered with the syringe cap later, as designed in Figure 3.4. Inside the outer tube, the inner tube was inserted, and this combined tube was placed in the middle of the glass slide horizontally. The end of each glass tubes was connected with syringe needles, as designed in Figure 3.4, to connect with polyethylene tubes during the experiment. Finally, these glass tubes and syringe needles were fixed on a glass slide with the help of epoxy resin and hardener. The chip was left for about 24 hours so that all these components get fixed. The microfluidic chip designed, prepared, and used in the laboratory is shown in Figure 3.5.

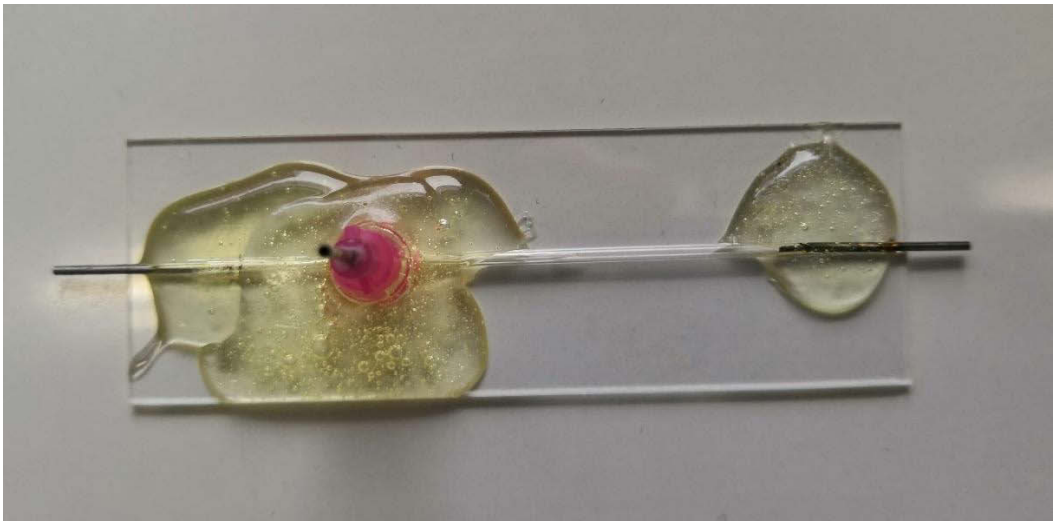

Figure 3.5 Picture of a microfluidic chip designed, prepared, and used in the laboratory.

3.7.2 Setup of microfluidics experiment

In order to carry out the microfluidics experiment, the protocol from Chen et al., 2015 was followed. All the microfluidics components (microfluidics pumps 1 and 2, microfluidic chip, and collecting glass vial) were set up as shown in Figure 3.6.

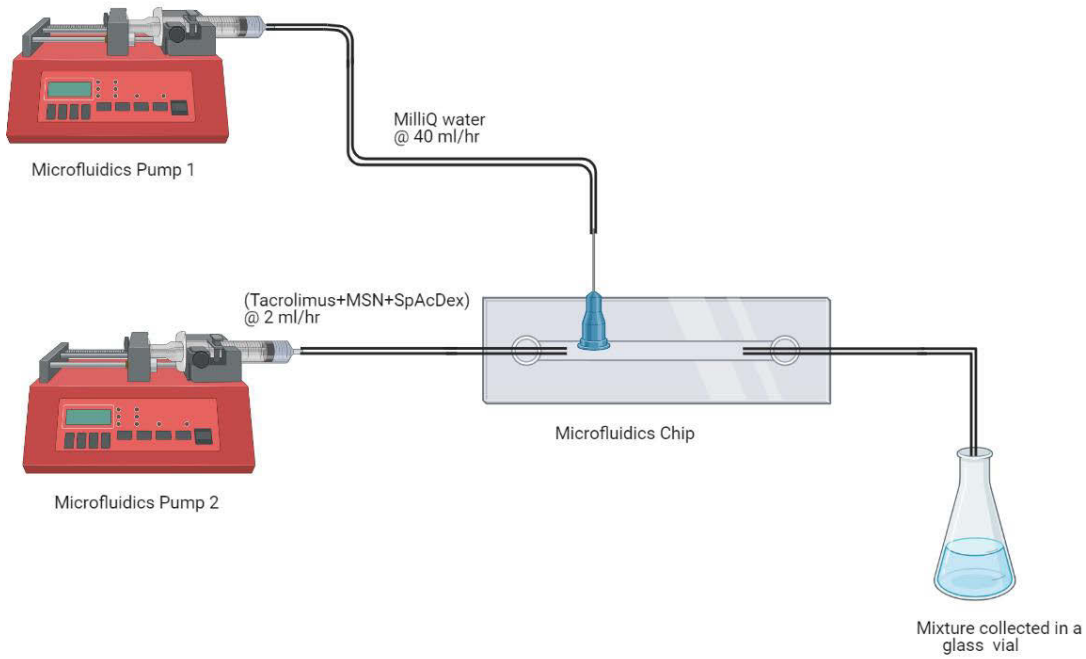

Figure 3.6 Schematic design of Microfluidics process

In order to carry out the microfluidics process, the inlet of the microfluidic chip was connected with a milliQwater syringe, while the outlet with tacrolimus encapsulated MSN with a polymer solution syringe. These connections were carried out with the help of polyethylene tubes (Scientific commodities INC, USA). The syringe solution had the mixtures of Tacrolimus, MSN, and SpAcDex solutions, in the ratio of 5:1:1 (Tacrolimus:MSN:SpAcDex = 5:1:1). Furthermore, the flow of these solutions was optimized at a different rate. The flow of MilliQ water was kept @ 40 ml/hour while the solution having a mixture of tacrolimus encapsulated MSN and SpAcDEx solutions @ 2 ml/hr. The flow of the solution was monitored with the help of a high-speed digital microscope (Dolomite Microfluidics, UK) situated just above the microfluidic chip.

The parameters including the number of frames and duration could be seen in the monitor. Figure 3.8 shows the flow of milliQ water solution passing through the microfluidic chip. The solution, which was mixed through the microfluidic chip was collected into a glass vial with the help of polyethylene tubes. The stirring magnet present in the glass vial helped further the mixing of the solution. Figure 3.7 shows the microfluidics system, along with its components used for this experiment.

Figure 3.7 Picture of Microfluidics machine used in the experiment (PMD, Harvard Apparatus)

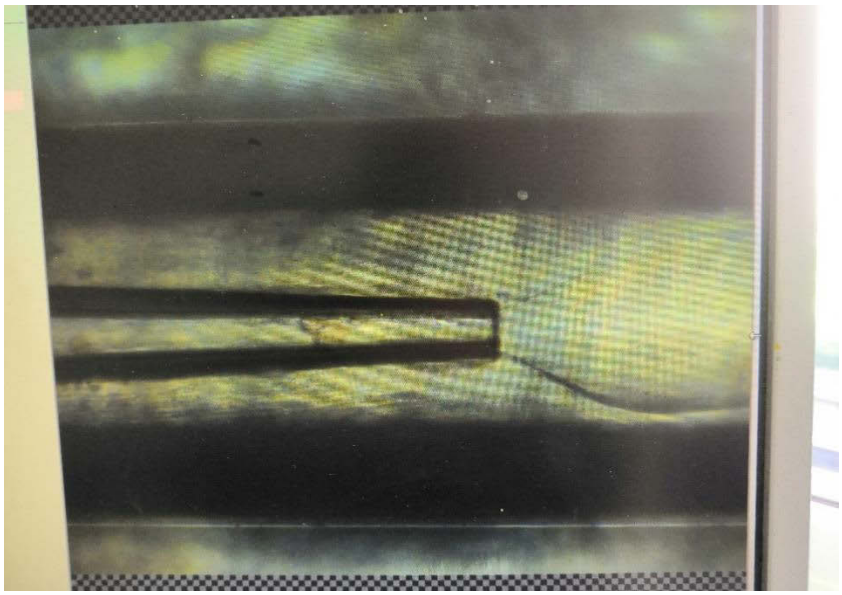

Figure 3.8 The flow of solution passing through the microfluidic chip and the bubble seen in the picture belongs to the milliQ water

After pumping out all the solutions from both pumps, they got turned off. Then the collected solution was centrifuged @ of 13,000 rpm for 5 min (Sorvall Lynx 4000 Centrifuge, Thermo Scientific). After all the steps, the extract got collected into another tube by taking away the supernatant. This final extract became the MSN-tacrolimus-SpAcDex complex.

3.8 In vitro cell viability and cytotoxicity measurement

In vitro cell viability and cell proliferation are types of parameters and are used to study the biological material attached to the nanoparticles. Furthermore, it helps to determine the toxicity of the nanoparticles against the living material. Hence, it is termed cytotoxicity. These cytotoxicity assays are based on either assessing damage to cellular membrane or cell viability or cell apoptosis or cell proliferation method. Here, for this study, a cell proliferation assay type was chosen. In addition, among varieties of cell proliferation assays, WST-1 cell proliferation assay was chosen and executed with HUVECs.

The WST-1 cell proliferation type of assay is precise, sensitive, reliable, non-radioactive, fast, accurate, inexpensive, and easy to execute. It is used to measure cell proliferation, cell viability, and cytotoxicity in mammalian cells. It is regarded as highly convenient because it does not require washing, harvesting, or solubilization of cells, and it can be conducted in single tissue culture. The protocol or principle of this assay is mainly based on the reduction of the tetrazolium salt WST-1 (pale yellow) to formazan (dark yellow) due to cellular mitochondrial dehydrogenases as shown in Figure 3.9. The formation of the dark yellow-colored formazan is measured at 420-480 nm (optimal at 440 nm), and it is directly related to the number of cells (G. BioSciences, 2013). In addition to these, if the number of viable cells is bigger, the activity of the mitochondrial dehydrogenase becomes higher, which further leads to a higher amount of formazan dye formation. Thus, the metabolically active cells cause the formation of formazan dye, and this dye can be quantified with the help of scanning multi-well spectrophotometer (Merck, 2020). Thus, it analyzes the number of viable cells with the help of cleavage of tetrazolium salts added to the culture medium. In addition, it compares the number of cells before and after the interaction with nanoparticles, which later becomes the key for cytotoxicity determination. In addition of these, this assay uses the 96-well-plate for cell culture (Merck, 2020).

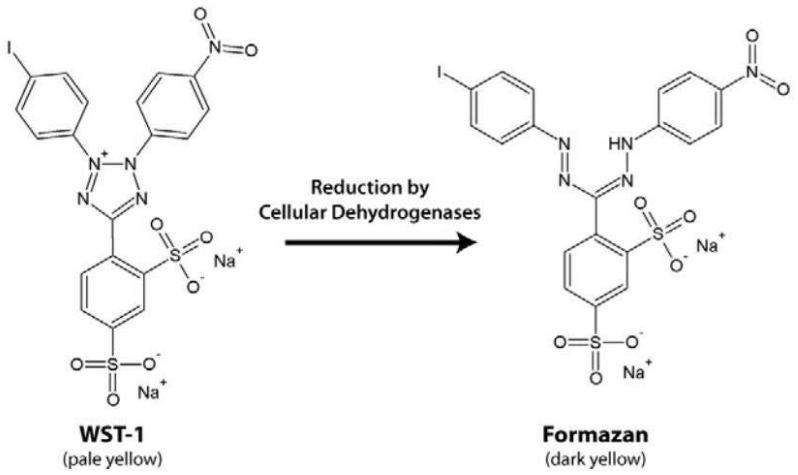

Figure 3.9 Transformation process of WST-1 to Formazan during WST-1 assay (G. BioSciences, 2013)

The assay was carried out by following the protocol from the manufacturer's instructions. In a brief, first, the HUVECs were seeded in a 96-well plate and incubated in cultured medium for 24 hours at 36.5^0C with 4.6% CO_2 (Hera Cell, Heraeus). The cultured medium was buffered with Phosphate-buffered saline (PBS) (BioWhittaker, Lonza). Once they were cultured and grown to 80-90% confluency, they were exposed to the serial concentration of MSN and MSN-tacrolimus-SpAcDex complex along with the WST-1 reagent and the Dimethyl Sulfoxide (DMSO). These serial concentrations were 5 mg/ml, 10 mg/ml, 15 mg/ml, 20 mg/ml, and 100 mg/ml. The main purpose of adding DMSO is to restrict the further growth of HUVECs. Besides these nanoparticle and nanoparticle complex exposed cells, a group of cells (blank or negative) were skipped or untouched with any reagents (except DMSO) in order to compare the result with the group of cells exposed to nanoparticles and nanoparticle complexes. Each concentration was replicated 5 times, and this 96-well plate was left for 2 hours.

After 2 hours, the color of the cell inside the plate changed from pale yellow to dark yellow, and the absorbance of Formazan got detected with the help of a multi-well spectrophotometer (Varioksan Flash, Thermo Fisher Scientific) at 440 nm. The absorbance data obtained from the spectrophotometer got calculated and analyzed to determine the cell viability and cytotoxicity of the MSN and MSN-tacrolimus-SpAcDex complex.

In order to determine the cytotoxicity, first, the cytotoxicity in each well needed to be calculated. For this, the culture medium background (blank or negative one) was subtracted from the assay result, and the actual cytotoxicity in percentage was calculated with the following formula.

$$\%\ cytotoxicity = \frac{(cell\ experiment - cell\ blank)}{(cell\ experiment)} \times 100$$

After getting the cytotoxicity values of each well, the overall cytotoxicity of MSN and MSN-tacrolimus-SpAcDex complex was calculated.

3.9 Imaging

The laboratory synthesized MSNs and CuS@MSNs were observed under a Transmission Electron Microscope (TEM). Similarly, a Confocal microscope (CFM) was used to observe the cell viability assay and the determination of cytotoxicity.

3.9.1 Transmission Electron Microscopy

Transmission Electron Microscope (TEM) uses the interaction of coherent electron beams to examine the morphology and composition in fine detail, which finally produces high-resolution images. Thus, it uses electrons as a source of illumination, unlike in typical light microscopes, where the light beam plays a source of illumination. Furthermore, it is different than the Scanning Electron microscope (SEM). The SEM strikes an electron beam on the sample surface and detects secondary electron signals, and these signals are used to form images. However, in TEM, an electron beam penetrates the samples and gives the projection view of the sample. These electrons have a very short wavelength and possess high energy. That is the reason that they can penetrate the thin sample. Furthermore, the sample or specimen must be ultrathin so that electrons must pass through it without any significant energy loss.

As mentioned above, the beam of electrons must be coherent, and these coherent beams of electrons will be produced only when the working voltage is too high (1000's of volts). Therefore, electron microscopes are usually equipped with 50-200 kV of accelerating voltage (Williams and Carter, 1996).

The series of lenses present inside the electron microscope can highly magnify the transmitted and scattered electrons. This magnification results in the formation of high-resolution images.

In order to observe the MSN under TEM, first, 0.1 ml solution of synthesized MSN, having 0.5 mg/ml of concentration strength, was dropped on an ultrathin copper grid of TEM sample holder. It was left for around 1 hour so that all ethanol will evaporate. After evaporation of ethanol, only MSNs were present on the grid, and this grid was inserted

into the TEM (JEM-1400 Plus Electron Microscope, JEOL Japan). After this, the images got started to display on the screen. The TEM used in this study has an accelerating voltage of 80 kV, and its picture is shown in Figure 3.10.

Figure 3.10 Picture of an Electron Microscope (JEM-1400 Plus Electron Microscope, JEOL Japan) used for the observation of nanoparticles

3.9.2 Confocal Microscopy

The confocal microscope (CFM) used for this study will be the Laser scanning one. Generally, the confocal microscope uses fluorescence optics as a source of illumination, as in other widefield microscopes. However, it has more advantages over the latter one. The confocal one focuses on a defined spot at a specific depth within the sample, but the widefield one illuminates the whole sample at once. The focusing of laser light at a certain point causes the emission of fluorescent light in the same place. In addition, a pinhole situated at the optical pathway cuts off signals that are out of focus and lets fluorescent signals enter only from the focused point (Fellers and Davidson, 2020).

It scans the specimen in a raster pattern so that images of one single optical plane are created at once. As it scans several optical planes in a different timeframe, it can be also used for thick specimens. In addition, after scanning all the optical planes, it can create 3D images. Besides these, it is possible to analyze the multicolor immunofluorescence staining with the help of a confocal microscope as it comprises several lasers, along with several emission and excitation filters (Ibdi, 2020).

For the present study, the primary purpose of carrying out confocal microscopy imaging was to validate the cellular uptake of the MSN-tacrolimus-SpAcDex complex by HUVECs. During this procedure, 3 sets of the Petri dishes containing HUVECs were

taken. These were labeled with ‘A’, ‘B’, and ‘C’. The dish ‘A’ was supposed to fix after 2 hours, while the dish ‘B’, 6 hours, and the dish ‘C’, 24 hours. All of these Petri dishes were fixed with MSN-tacrolimus-SpAcDex complex and fluorescent particles. For this process, the reagent Paraformaldehyde (PFA) (BioWhittaker, Lonza) helped to fix the cells and the nanoparticle complexes together. The fluorescent particle used in this process was Cyanine 5 (Cy5). It is a bright far-red fluorescent dye and has 650 nm of excitation and 670 nm of emission wavelength. After fixing the cells, their growth was supposed to stop, and these were further stained with 4′,6-diamidino-2-phenylindole (DAPI). DAPI was used to stain nucleic acid for fluorescence microscopy and helped to determine the number of nuclei and assess gross cell morphology (Merck, 2020). Finally, all of these Petri dishes were observed with a laser scanning confocal microscope (Zeiss LSM780, Zeiss), and the images seen through the microscope were also captured. The objective lens used was 20x, 40x, and 63x. Furthermore, as the captured images were raw, they were further processed and analyzed with the help of Zen Lite software (Zen 3.3, Carl Zeiss Microscopy).

4. Results

4.1 MSNs under Transmission Electron Microscope (TEM)

The laboratory synthesized MSNs were observed with the help of TEM. They were spherical in size and about 50 - 80 nm in diameter. Furthermore, there were clear mesoporous structures, and these mesoporous structures were arranged in order. The empty channels around the core were also seen clearly. These empty channels were the place where tacrolimus will be placed during loading. Figure 4.1 shows the structure of MSNs under TEM.

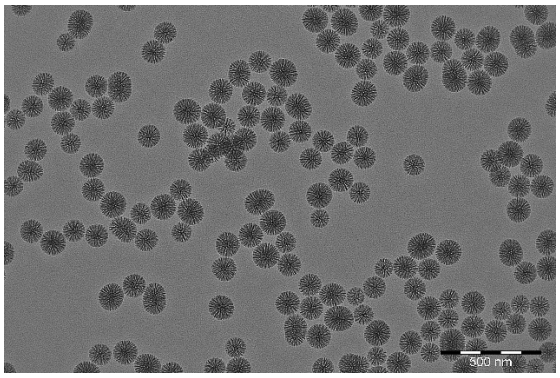

(A)

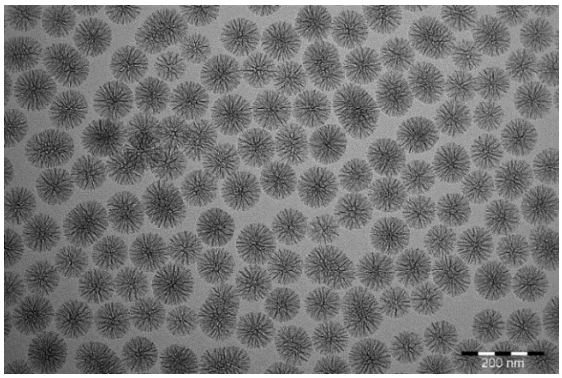

(B)

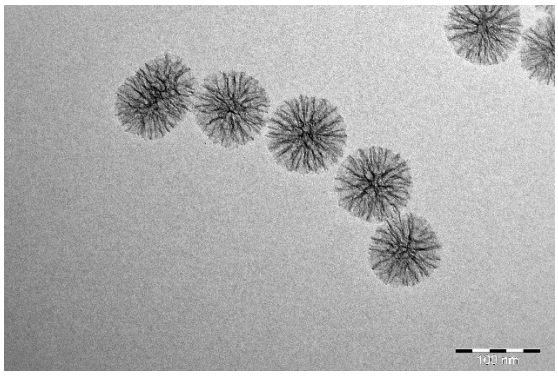

(C)

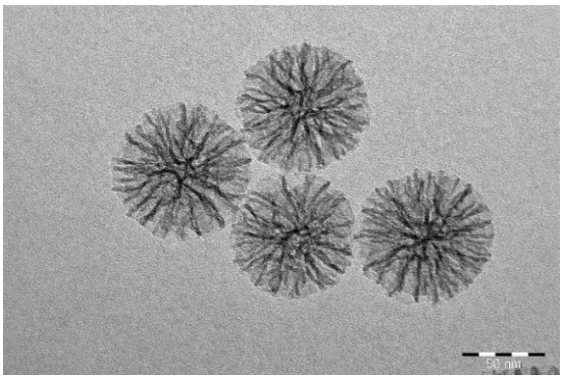

(D)

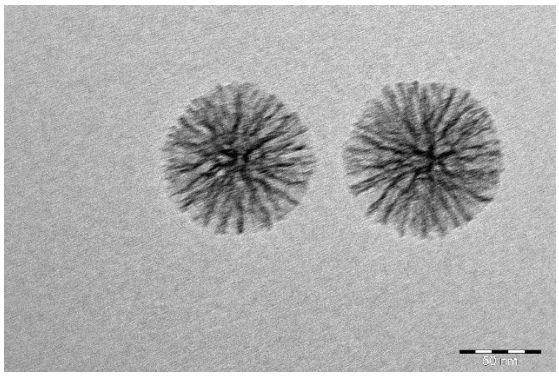

(E)

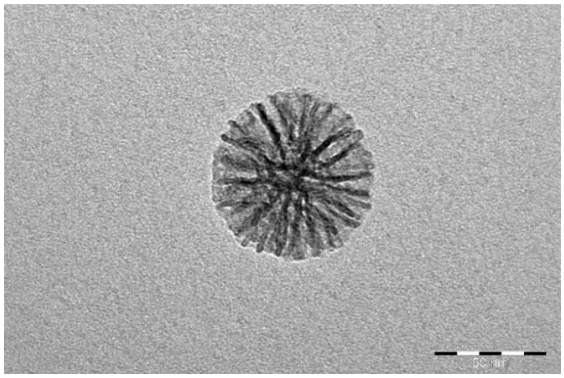

(F)

Figure 4.1. (A - F) MSNs seen under TEM. They were spherical in shape and the mesoporous structure of MSNs can be seen under high zoom. Scale bar = 500 nm (A), 200 nm (B), 100 nm (C) and 50 nm (D), (E) and (F)

4.2 CuS@MSNs under Transmission Electron Microscope (TEM)

After synthesis of CuS@MSN, they were observed under TEM. According to Figure 4.2, the CuS@MSN contains CuS as core material and the MSN as an outer sphere. In addition to the spherical ones, they were found in other shapes too, such as rod-shaped. Some of these nanoparticles were found alone, some aggregated together, and some formed a cluster. The size of these nanoparticles varied from 50 - 120 nm.

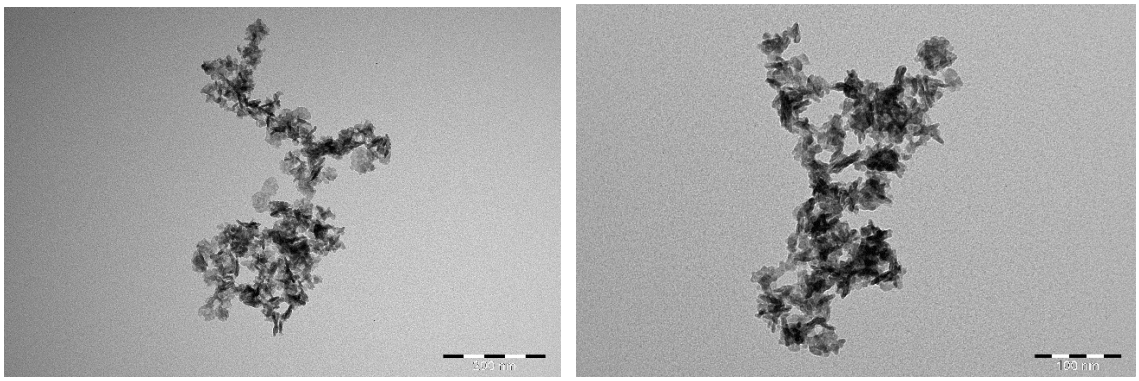

(A) (B)

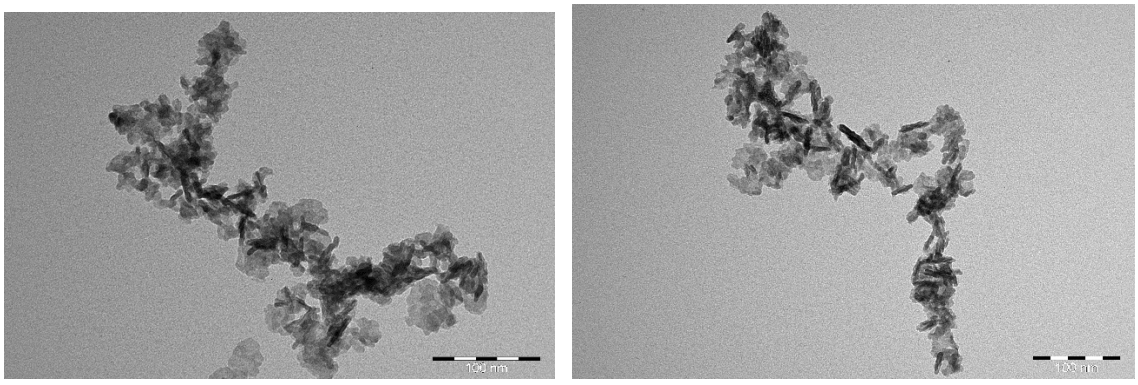

(C) (D)

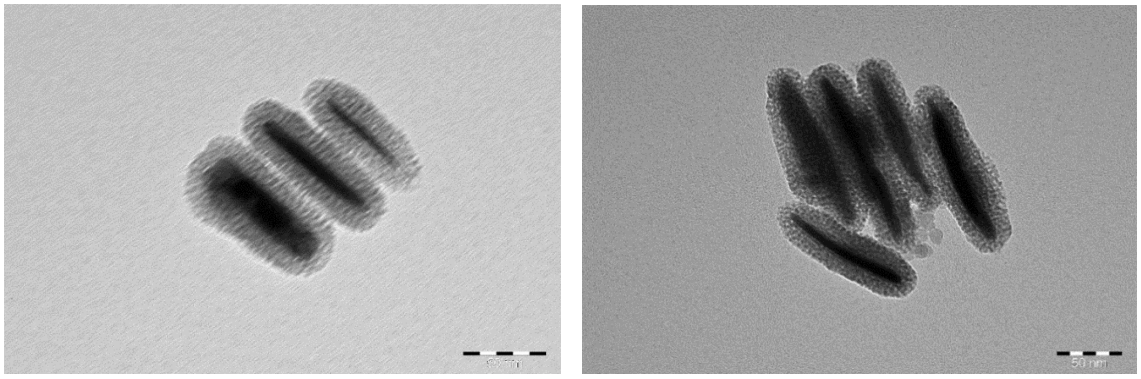

(E) (F)

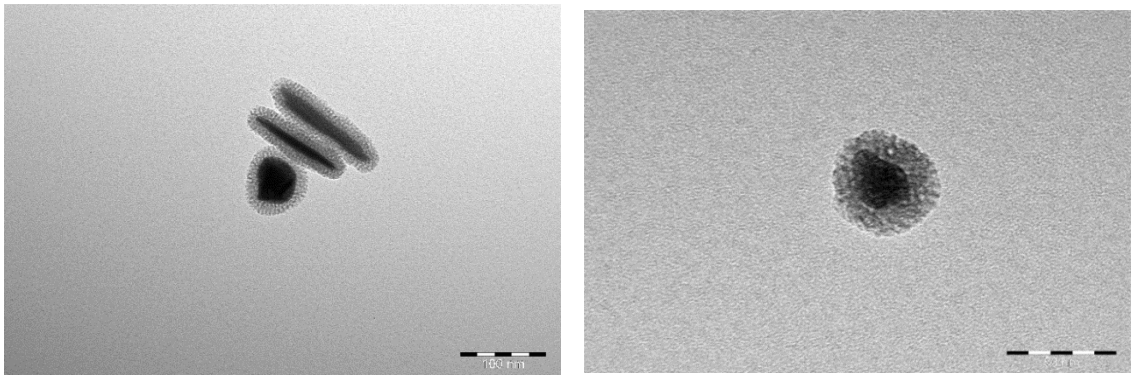

(G) (H)

Figure 4.2. (A - D) Aggregated CuS-CTAC nanoparticles. (E - H) CuS@MSN nanoparticles. Some of these are rod and spindle in shape while some are spherical. In these nanoparticles, CuS can be seen as a central core while the MSN as an outer sphere. These nanoparticles were observed under TEM. Scale bar = 200 nm (A), 100 nm (B), (C), (D) and (G), 50 nm (E), (F) and (H)

4.3 Loading of Tacrolimus with MSNs

After the measurement of the UV ray intensity of tacrolimus, the data were collected. The data included the concentration of the tacrolimus, the value of UV ray intensity (average), and the standard deviation. The data are shown in table 4.1 and with the help of these data, the graph was drawn as shown in Figure 4.3.

Concentration (mg/ml)	UV ray intensity (in average)	Standard deviation
0.1	0.265	0.022
0.2	0.475	0.027

0.3	0.663	0.024
0.4	0.855	0.022
0.5	0.949	0.042

Table 4.1 Data showing UV ray intensities and standard deviation, with respect to the MSN concentration.

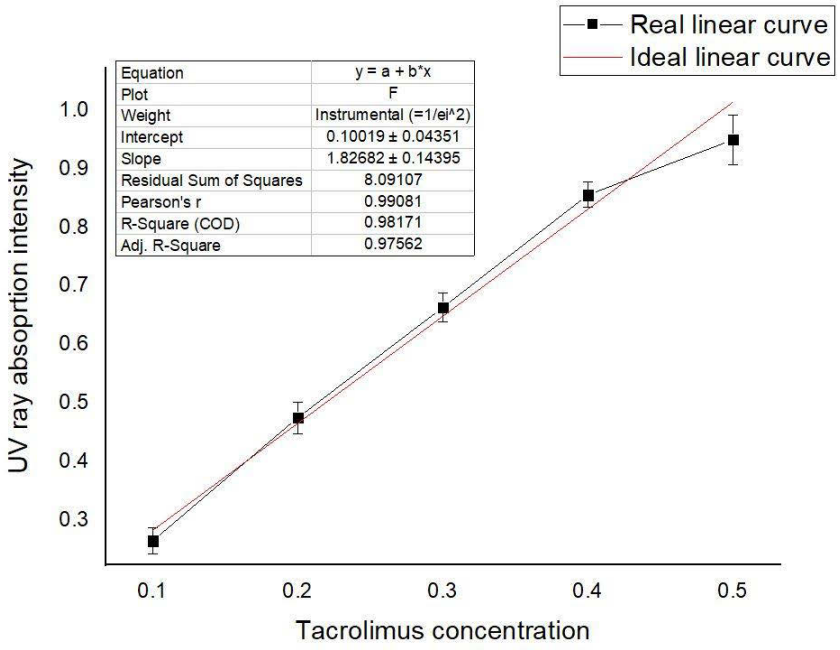

Figure 4.3 A graph showing the relationship between tacrolimus concentration and UV ray absorption in the form of intensity curve. The UV ray absorption intensity method helps to quantify the particles present in the solution and thus, determines the concentration strength of the solution.

In the graph of Figure 4.3, the black line shows the actual UV ray intensity absorption by tacrolimus, while the red line is the ideal one (used for fitting with linear one). Thus, it shows that the UV ray intensity absorption by different concentrations of tacrolimus solutions (from 0.1 mg/ml to 0.5 mg/ml) followed the linear curve. In addition, with the help of the graph, the actual concentration of tacrolimus solution, synthesized in the laboratory, was calculated.

The actual amount of tacrolimus loaded in MSNs was dependent on the concentration of MSNs and calculated by the following formula.

Amount of tacrolimus loaded in MSN =

Before loading concentration – After loading concentration

Furthermore, Table 4.2 shows the data of tacrolimus loaded in different concentration strengths of MSN.

Tacrolimus:MSN ratio	Before loading concentration in mg/ml (A)	After loading concentration in mg/ml (B)	Net loaded amount (A - B) mg/ml
1:1	0.988129455	0.934569455	0.05356
2:1	1.80423229	1.789978562	0.014253728
3:1	2.702975561	2.750138631	-0.04716307
4:1	3.20810252	3.081000429	0.127102091
5:1	**4.644733457**	**4.017035873**	**0.627697585**
6:1	5.155558096	5.06397599	0.091582107

Table 4.2 Data showing the amount of Tacrolimus loaded in MSN with respect to the MSN concentration.

As seen in Table 4.2, it was found that the 5:1 ratio of tacrolimus and MSN has the highest loaded amount, among other ratios. Thus, these findings show that approximately 63% of tacrolimus will be loaded into MSN when 5:1 ratio tacrolimus and MSNs are used.

4.4 Zeta potential measurement of MSN

The zeta potential measurement of MSN alone showed a negative charge. At 0.5 mg/ml concentration, the average value was -15.1 mV with standard deviation of 0.513, while at 0.25 mg/ml concentration, it was found to be -19.6 mV with standard deviation of 0.854. The higher the concentration, the higher the value will be negative. The detail values are shown in table 4.3.

Concentration strength	First time (in mV)	Second time (in mV)	Third time (in mV)	Average (in mV)	Std. Dev.
0.25 mg/ml	-19.5	-18.8	-20.5	-19.6	0.854
0.5 mg/ml	-15.2	-14.5	-15.5	-15.1	0.513

Table 4.3 Zeta potential values of MSN alone.

Similarly, from table 4.4, it is shown that the zeta potential value of tacrolimus loaded into MSN in the ratio of 5:1 at 0.5 mg/ml concentration was -15.5 mV on average with 0.473 of standard deviation.

Concentration strength	**First time (in mV)**	**Second time (in mV)**	**Third time (in mV)**	**Average (in mV)**	**Std. Dev.**
0.5 mg/ml and (5:1=Tacrolimus: MSN)	-15.0	-15.7	-15.9	-15.5	0.473

Table 4.4 Zeta potential value of tacrolimus and MSN solution in 5:1 ratio

4.5 Microfluidics

After carrying out the microfluidics experiment, the tacrolimus-loaded MSNs got further encapsulated by SpAcDex polymer to form the MSN-tacrolimus-SpAcDex complex. This MSN-tacrolimus-SpAcDex complex is now ready for further research. The SpAcDex polymers cover the MSN-tacrolimus complex from the outside and give more stability.

4.6 In Vitro Cell Viability and cytotoxicity measurement

After the calculation of *in vitro* cell viability and cytotoxicity with the help of absorbance values of respective well plates through WST-1 assay, the actual cell viability was obtained. A graph was drawn using the data obtained from cell viability in percentage and both the MSN and the MSN-tacrolimus-SpAcDex complex concentration strengths. The graph is shown in Figure 4.4, where the x-axis represents the concentration strengths of MSN and MSN-tacrolimus-SpAcDex, while the y-axis, the cell viability in percentage.

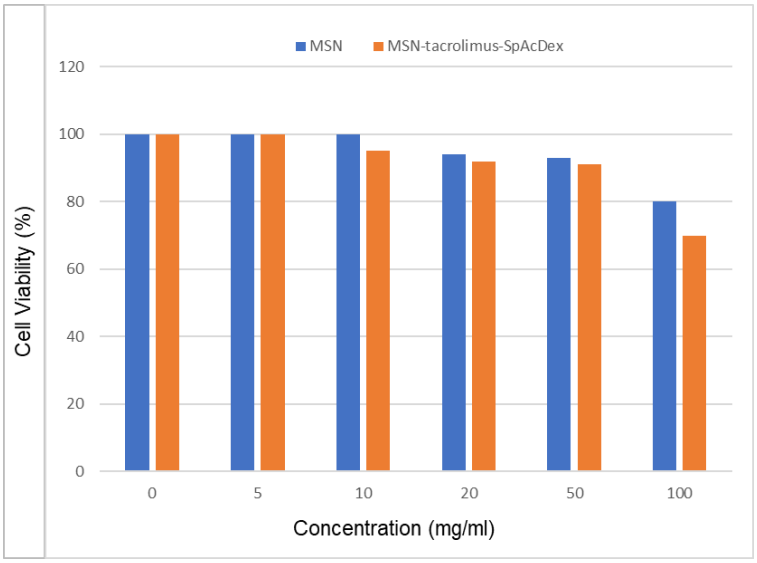

Figure 4.4. The graph showing the relationship between the concentration of MSN, MSN-tacrolimus-SpAcDex and HUVECs viability. The HUVECs were treated with either nanoparticles or nanoparticle-drug-polymer complexes for about 2 hours.

As we can see in the graph of Figure 4.4, there was almost no cytotoxic effect up to the use of 50 mg/ml of both MSN and MSN-tacrolimus-SpAcDex complex as the cell viability till this concentration was nearly more than 90%. After using more than 50 mg/ml concentration, cell viability got decreased. It means the cytotoxic effect of these nanoparticles and nanoparticle complexes on HUVECs got started after using significantly high concentrations (around 100 mg/ml). However, the maximum cytotoxic effect shown was approximately 30% only.

4.7 Cells under Confocal Microscope (CFM)

As the main purpose of the confocal microscopy in the present study is to confirm the cellular uptake of the MSN-tacrolimus-SpAcDex complex, a series of images were taken with the help of laser scanning confocal microscope. Those images were presented in Figure 4.5. So, Figure 4.5 showed the real situations of nanoparticle complexes uptake by HUVECs. Figure 4.5 is started with a cellular uptake image at 2 hours @ 40x (image 'A'). From these images, it can be confirmed that the up-taking process already took place in 2 hours, as an image ('A') showed a little bit of red-colored dots. These dots were from the fluorescence particle (cyn5), and these are associated with the nanoparticle complexes. As time increases, concentration strengths of nanoparticle complexes were also in the increasing trend. It caused the appearance of more red-colored dots in images from both 6 hours and 24 hours than that of 2 hours. Therefore, images ('A') and ('B') comprised the lowest concentration of MSN-tacrolimus-SpAcDex complex, while images ('E') and ('F'), the highest one.

The blue color seen in all these images was signals from DNA that was stained with DAPI.

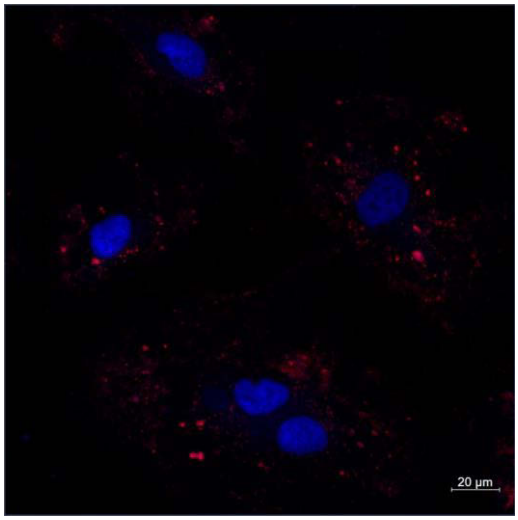

(A)

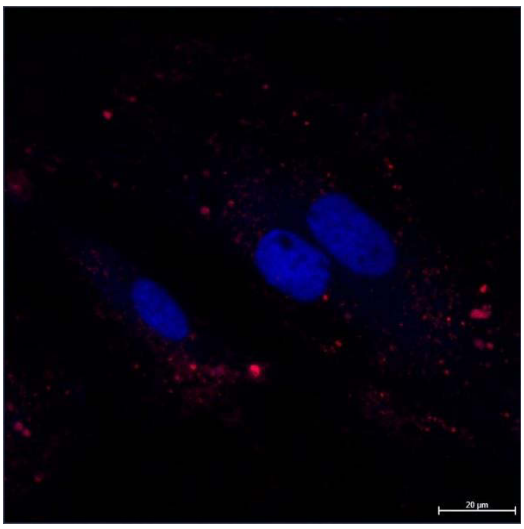

(B)

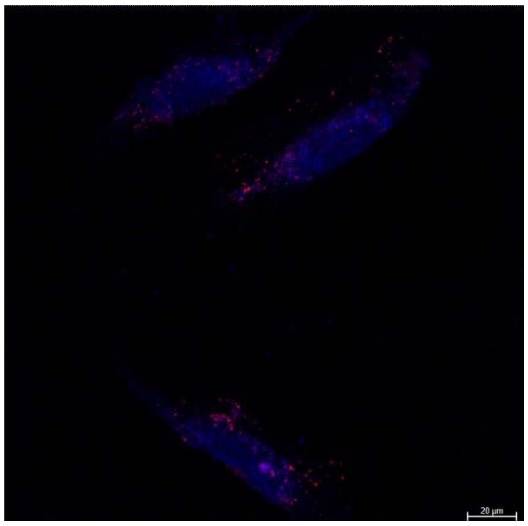

(C)

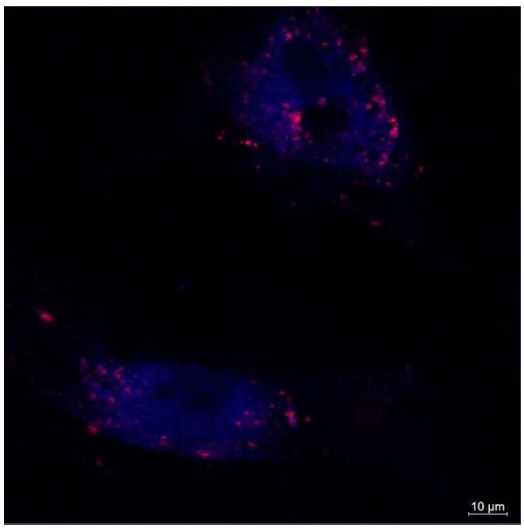

(D)

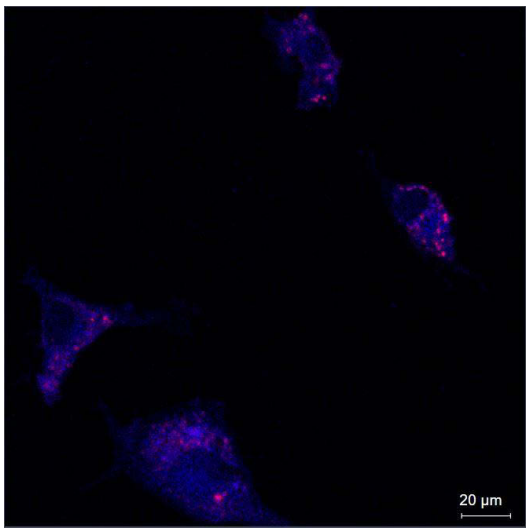

(E)

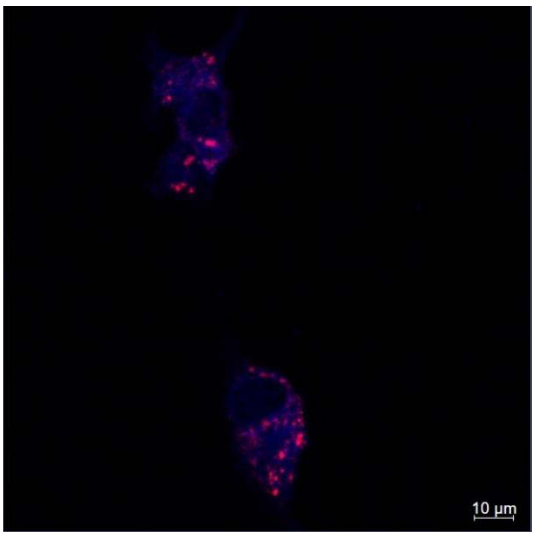

(F)

Figure 4.5 HUVECs observed under Confocal microscope. The red color is showing the uptake of MSN-Tacrolimus-SpAcDex complex by HUVECs in different timeline. (A) 2 hr @ 40x (B) 2 hr @ 63x (C) 6 hr @ 40x (D) 6 hr @ 63x (E) 24 hr @ 40x (F) 24 hr @ 63x. The blue color is from DNA that was stained with DAPI. Scale bar = 20 µm (A), (B), (C) and (E) and 10 µm (D) and (E)

5. Discussion

Nanomaterials and nanoparticles are any substances with one of the dimensions in nanoscale. The synthesis of these nanoparticles in the laboratory does not possess complicated techniques and is not time-consuming. MSN and CuS@MSN are examples of nanoparticles. The particles at the nanoscale level possess unique characteristics that are not present at their macroscale ones. These unique characteristics could be used for different purposes in different fields. Among these purposes, drug delivery is one of the interesting features, where the drug is loaded with nanoparticles and delivered to specific sites.

End stage renal disease is the last stage of kidney disease where the kidney needs to be replaced with a new one as the patient's kidney cannot work as normal anymore. However, after the kidney replacement, there is always a risk of kidney failure as the host's immune system recognizes the transplanted kidney as a foreign agent and tries to kill it all the time. The best treatment of this problem is to kill the host's immune cells present in the kidney with tacrolimus and methylprednisolone drugs. Therefore, it would be a great solution if these drugs could be loaded into nanoparticles and delivered directly into endothelial cells of the kidney. This is the reason why we have chosen MSNs and tacrolimus drugs.

This thesis study was executed in order to know more about MSNs. Thus, we hypothesized that the laboratory synthesis of nanoparticles is easy, and the MSN has a good tacrolimus loading capacity with no significant cytotoxic effect. During the study, the drug loading capacity and the efficiency of MSNs with tacrolimus drug were analyzed. Furthermore, both the nature and the value of electric charges, present on the surface of MSN alone and tacrolimus loaded MSN, were also calculated. Furthermore, the cytotoxic effect of both the MSNs and the MSN-tacrolimus-SpAcDex complexes was figured out. However, during the cytotoxic test (assay), HUVECs were used instead of actual endothelial cells of a kidney because both cells resemble each other to a greater extent. In addition, the availability of HUVECs was higher and easier compared with endothelial cells of the kidney.

5.1 Synthesis of MSN and CuS@MSN in the laboratory is easy and the outcome is good

The synthesis of MSN and CuS@MSN in the laboratory is easy, and the whole procedure for both nanoparticles comprises a few steps which are to be followed in order. The procedure steps of MSN synthesis were followed from the protocol of Shen et al. (2014), while the CuS@MSN one from the Chen et al. (2015) one.

Shen et al. (2014) synthesized hollow MSNs along with pores in a variety of sizes. According to them, the manipulation of TEOS concentration in cyclohexane gives rise to different sizes of MSNs, ranging from 5 - 180 nm. In our study, the range of hollow MSNs found was about 50 - 80 nm using TEOS in Cyclohexane 10%v/v, and the size of the MSNs is similar to that of the study by Shen et al. (2014).

In addition, the suspension method gives MSNs in a stable colloid solution in a concentrated amount with a size of approximately 50 nm (Wu et al., 2013). Both the condensation rate and the pH value affect the diameter of MSNs as Qiao et al. (2009) found MSNs of different sizes (30-85 nm) by the manipulation of those parameters. In addition, the method which uses Cetyltrimethyl ammonium bromide (CTAB) as an ingredient produces bigger-sized MSNs as 600-700 nm-sized MSNs were synthesized by Vazquez et al. (2017), who have used additional CTAB during the synthesis of MSNs. Yang et al. (2020) confirmed the size of synthesized MSNs of about 60 nm with the help of TEM and SEM during their experiment. Ngamcherdtrakul et al. (2018) synthesized the MSNs after the same protocol as in this study, where they got the MSNs with an average size of 50 nm. Furthermore, these synthesized MSNs were successfully used as nanocarriers.

Similarly, the CuS@MSNs, synthesized by Chen et al. (2015), have an average particle size of 65 nm. Furthermore, they changed the amount of CTAC (25 wt % solution) from 2 gm (or ~20 mg/mL by concentration) to 0.5 gm (or ~5 mg/mL by concentration) and found nanoparticles of the size of 30-40 nm. Here, our study, which follows the same protocol, got 50-120 nm-sized nanoparticles by using 2 gm CTAC.

During the synthesis of CuS@MSN, Lu et al. (2019) found the sizes of nanoparticles of 33 nm, 44 nm, and 48 nm, when the amount of TEOS used was 170 ml, 180 ml, and 200 ml, respectively. In our study, the amount of TEOS used was 200 mL and got similar-sized nanoparticles. Yang et al. (2020) found the size of CuS@MSN of around 85 nm under TEM. Similarly, with the help of TEM, the hydrodynamic diameter of CuS@MSN was found to be approximately 70 nm in the experiment carried out by Wu et al. (2014). In addition, the average hydrodynamic diameter measured by Lu et al. (2015) was 49.5

nm. This size is excellent for passively targeting solid tumors, and in our case, we got the size of CuS@MSN under the same suitable range.

It is said that nanoparticles with a diameter below 300 nm are suitable to use as nanocarriers for drug delivery systems because these ranges of nanoparticles are easily taken up into cells. In addition, nanoparticles that are bigger than this range may stimulate an immune response and would not be as effective as they are supposed to be (Karimi et al., 2016). Thus, after comparing the other's results of the same type of experiment with our one, it was found that our synthesized nanoparticles can be considered as good nanoparticles as they are well below 300 nm and in good shape. These nanoparticles can be used for different purposes, including nanocarriers in drug delivery systems. Moreover, the whole procedure to synthesize nanoparticles (both the MSN and the Cus@MSN) is easy and yields a good amount of nanoparticles.

5.2 Loading of tacrolimus into MSN is easy, convenient, low cost and has significantly higher efficiency

In the present study, tacrolimus is the drug that loaded into the MSNs. The amount and easiness of the tacrolimus loading process depend upon the type of nanocarriers and methods. For example, Liu et al. (2016) loaded the drug tacrolimus into MSN, along with other lipids excipients, and found out that the drug loading process was simple, low cost, ecological, and easy to obtain at an industrial scale.

During the experiment executed by Paiva et al. (2020), they got the result of tacrolimus loading into MSN with 3-aminopropyltriethoxysilane (MSN-APTES) as 7%. Similarly, Khan et al. (2016) revealed the significantly high solubilization of tacrolimus through *in vitro* lipolysis studies and the use of aqueous phase of nanostructured lipid carrier (NLC), and the result was 69.3%.

In some cases, the rate of tacrolimus loading was strange. For example, Lamprecht et al. (2005) got the result of less than 1% of tacrolimus loading in nanoparticles at room temperature. But, under an ice bath, they found that it was around 40%. In our experiment, we got approximately 63% loading of tacrolimus in MSN, under the 5:1 ratio of tacrolimus and MSN. In addition, our drug loading experiment did not need any extra lipid or carrier to enhance the loading. The drug was simply loaded by stirring and further encapsulated with SpAcDex through microfluidics.

It is also found that a different nanocarrier than MSN, such as Peptide-Decorated PEG−PBG (PEP-PEG-PBG) polymer, could encapsulate the tacrolimus drug at the rate of 60% when using 4:1 ratio (tacrolimus:PEP-PEG-PBG). In addition, this amount was

considered a relatively high amount compared with other polymeric micelles. (Lin et al., 2019). Likewise, Harun et al. (2021) successfully loaded the moderate amount of Ruthenium Polypyridyl drug into MSN and called it an ideal method for drug delivery. In our experiment, we loaded a significantly good amount of tacrolimus drug, and thus we can consider MSN as an excellent carrier for drug delivery.

The tacrolimus-MSN loading process of this study can be considered as easy and convenient. First, it got higher loading efficiency of approximately 63%. This efficiency was obtained by using the MSN and the tacrolimus in the ratio of 1:5, only by stirring @ 300 rpm for 24 hours. In addition, it is a low-cost method as it does not need any complicated method or special apparatus for stirring purposes. Second, the experiment was conducted at normal room temperature.

Since it is a novel approach and tried for the first time, there could have been several factors, which directly or indirectly can affect the loading of tacrolimus. As it was seen in the experiment, the mixture-stirring time and the temperature in the loading process are crucial factors. Thus, manipulation of these factors could have given a different result than the one we got in our study.

5.3 The value of zeta potential determines the physical stability of MSNs

The physical stability of the nanoparticle depends upon the electric charge over its surface, and this electric charge is called zeta potential. In addition, this electric charge could be either positive or negative. Furthermore, it is found that the bigger the value of electric charge (could be positive or negative), the more stable the particle and vice versa. (Lu and Gao, 2010). Here, the same principle applies to MSN too. As zeta potential values ranging from -10 mV to +10 mV are considered as lower threshold range (neutral), nanoparticles (MSN too) with zeta potential value more than this range are considered as good and physically stable (Joseph and Singhvi, 2019).

Vazquez et al. (2017) team found the zeta potential value of MSN around 40 – 45 mV in their study, and due to its bigger value, they called it super stable MSN. Similarly, -30.7 mV by Luo et al. (2014) and -30 mV by Perez (2019) were recorded as zeta potential values of MSN, and these MSNs are stable too. Kim et al. (2021) synthesized the different sizes of MSNs by using the ingredients in different amounts. They also found different values of zeta potential, ranges from -9.3 to +25.7 mV. The study conducted by Luo et al. (2014) showed that the zeta potential of MSN was around -23 mV. In our experiment, we found different zeta potential values from different concentration strengths of MSNs, and these values are ranged from -15 mV to -20 mV. As the zeta

potential values of MSNs from our experiment are higher than the lower threshold range, these MSNs can be considered as good and physically stable ones.

Lin et al. (2019) succeeded in the encapsulation of tacrolimus with PEP−PEG−PBG-derived nanomicelle, along with good loading efficiency in their experiment. In addition, before encapsulating the tacrolimus, they found the zeta potential value of PEP−PEG−PBG-derived nanomicelle +14 mV. In addition, they mentioned the nanomicelle physically stable. Likewise, Zhang et al. (2021) found the zeta potential value of amino-derived MSN (MSN@NH2) as +35 mV, and it was also physically stable.

Another team, Paiva et al. (2020), found varieties of zeta potential values from MSN and its derivatives. They found a zeta potential value of MSN around -25mV, MSN-APTES around +30 mV, and MSN-APTES-tacrolimus around +33 mV. But, in our study, the zeta potential value of MSN (0.5 mg/ml concentration) was around -15 mV, and the zeta potential value of MSN-Tacrolimus (both have 0.5 mg/ml concentration) was also the same. Despite the differences in zeta potential values of the study done by Paiva et al. (2020) with our one, it can be said that the tacrolimus does not pose any significant electric charge. The change in zeta potential value in the study of Paiva et al. (2020) was due to the modification of MSN with APTES. In our experiment, MSN was not modified with any group, and this group was responsible for the change in the nature and value of zeta potential. Thus, the loading of tacrolimus into MSN without modification did not affect the nature and value of zeta potential.

During an experiment carried out by Hu et al. (2017), the zeta potential value of MSN was found as -25 mV. However, the negative electric charge got reversed into a positive one, with +16.7 mV, after the modification with an amino group (-NH2). Furthermore, it again got reversed into a negative one, with around -29.6 mV, after the modification with a carboxyl group (-COOH). Likewise, He et al. (2017) noticed that the nature of electric charge from zeta potential of MSN reversed from around -23 mV to +23 mV after modifying with amino groups. Similarly, in the study of Sun et al. (2019), the zeta potential of MSN got reversed from around -22.6 mV to +24.3 mV after functionalizing with 3–aminopropyltriethoxysilane (APTES). The APTES comprises an amino group ($-NH_2$) as a dominant group.

In our experiment, MSN was used to load the tacrolimus drug, and even after loading, neither the zeta potential value nor the nature of the electric charge of MSN changed. Thus, we can say that the encapsulating or loading process is different from modifying or functionalizing process. In addition to these, modifying or functional groups present over the surface of MSN will determine the nature and amount of charge. However, the encapsulation process does not affect the nature or value of zeta potential at all.

5.4 MSNs and MSN-tacrolimus-SpAcDex complexes do not pose any cytotoxicity to HUVECs

The *in vitro* cell viability calculation and the cytotoxicity effect were conducted for both the MSN and the MSN-tacrolimus-SpAcDex. In addition, the type of test used for this experiment was WST-1 assay. Both the nanoparticles and the tacrolimus-loaded nanoparticles were tested separately.

According to Paiva et al. (2020), there is no cytotoxic effect of both the MSN-APTES, and the tacrolimus loaded MSN-APTES on ARPE-19 cells as the cell viability is more than 80%. In addition, they have used below 100 mg/ml concentration of tacrolimus-loaded MSN-APTES. In one of the researches of Zhang et al. (2021), it is found that the MSN has no significant cytotoxic effect on both *in vitro* and *in vivo* cases. They have used MSN with virus-mimicking nanoparticles. Likewise, bevacizumab nanoparticles loaded with MSN do not possess any *in vivo* toxicity (Sun et al., 2019).

The cytotoxicity test of MSN, with the help of a cell-based assay, found out that there is no cytotoxic effect of MSN on A549 cells (He et al., 2017) and MCF-7 cells (Kim et al., 2021), even at a higher concentration such as 200 mg/ml. Furthermore, the cell viability was more than 90%. However, there is evidence of cytotoxic effect with DOX loaded MSN (MSN-DOX) on A549 cells, according to He et al. (2017) but not with MCF-7 cells (Kim et al., 2021).

A study conducted by Harun et al. (2021) found that the ruthenium polypyridyl (Ru-PIP) complex loaded MSN (MSN-Ru-PIP) was highly toxic to various cancer cells. In addition, the doxorubicin and chlorin e6 loaded MSN with hyaluronic acid (MSN-HA-DOX-Ce6) was significantly toxic to squamous cancer cells (Park et al., 2019). That is why toxicity is also good in order to kill cancer cells properly. Furthermore, they termed this drug delivery method as an ideal method to treat various cancers.

So, from both of our and other's studies, we can say that the MSN alone is not cytotoxic when using lower than 200 mg/ml concentration. Similarly, the MSN-tacrolimus-SpAcDex complex is also not cytotoxic till the use of 50 mg/ml concentration. Only a negligible cytotoxic effect started to appear after using 100 mg/ml concentration of MSN-tacrolimus-SpAcDex complex. The reason behind it might be the toxicity of both tacrolimus and SpAcDex or either tacrolimus or SpAcDex, and it needs further study. Thus, the MSN and MSN-tacrolimus-SpAcDex complex are non-toxic but biocompatible. Furthermore, the nature of the assay does not affect the result of the cytotoxicity test.

6. Conclusion

In summary, mesoporous silica nanoparticles (MSNs), with pore size 50 - 80 nm and MSN dopped Copper Sulfide nanoparticles (CuS@MSNs), with pore size 50 - 120 nm, are synthesized successfully. Similarly, MSN shows a good tacrolimus drug loading capacity as it absorbs a significant amount of drug tacrolimus, and it is approximately 63% when using a 1:5 ratio of MSN and tacrolimus. In addition, both the MSN and the MSN-tacrolimus complex are stable as they have an average zeta potential of -15.1 mV and -15.5 mV, respectively. Furthermore, this MSN-tacrolimus complex can be encapsulated with SpAcDex polymer to form an MSN-tacrolimus-SpAcDex complex for further stability. Moreover, these MSNs and MSN-tacrolimus-SpAcDex complexes are not toxic to HUVECs. Thus, MSN can be loaded with tacrolimus and encapsulated with SpAcDex to target immune cells present in the patient's kidney. This type of tacrolimus delivery with the help of MSN@SpAcDex could be one of several methods to treat ESRD effectively. Thus, MSN, along with SpAcDex, has a great potential as a vector or carrier for different types of drugs in drug delivery methods.

7. Limitation of the study and Future work

The study was carried out to synthesize two different types of nanoparticles, viz., MSN and CuS@MSN, and separately load drugs (tacrolimus and methylprednisolone) into them, along with encapsulating with the SpAcDex polymer. In addition, it includes the cytotoxic testing of these nanoparticle-drug-polymer complexes. During the study, the synthesis of both types of nanoparticles was completed. In addition, the loading of tacrolimus into MSN was also got possible, along with its encapsulation with the SpAcDex polymer to form the MSN-tacrolimus-SpAcDex complex. Moreover, the cytotoxicity test of both the MSN and the MSN-tacrolimus-SpAcDex complex was also completed. However, the loading of methylprednisolone into CuS@MSN and encapsulating it with SpAcDex polymer, along with its cytotoxic test, were not possible to carry out. The main reason behind this was the insufficient time as the project was big enough for the master's thesis. Besides this, the pandemic situation due to the novel coronavirus caused the closing of laboratories and later restriction in Biocity building, due to which doing experiments in Biocity building was not possible and increased the whole study time. All of these made the pace of the project slow.

Thus, the future work of this study includes the loading of methylprednisolone into CuS@MSN and encapsulated with the SpAcDex polymer to make CuS-MSN-methylprednisolone-SpAcDex complex. Furthermore, the cytotoxic assay of both the nanoparticles and the nanoparticle complexes could also be done. Similarly, since the WST-1 assay was carried out with HUVECs, another future work could be the carrying out cytotoxic assay with the actual endothelial cells of the kidney. It will further clarify the relationship between the endothelial cells of the kidney and drug-loaded nanoparticles.

8. Acknowledgements

I would like to express special thanks of gratitude to my supervisor, Associate Professor Dr. Hongbo Zhang (Precision Nanomedicine group), who gave me the golden opportunity to do this wonderful thesis work. In addition, I am so grateful to Professor Jessica Rosenholm as I could carry out my experiments mainly in her Microfluidics and Cell Biology lab, which are situated in the Biocity building, 3rd floor. Besides this, I want to thank my lab supervisor Chang Liu for guiding and supporting me when I got lost during the planning and executing of the experiments.

I am also thankful to our BIMA teacher-tutor, Associate Professor Diana Toivola, whose suggestions and guidance were a lot for me during my thesis work. Furthermore, a big thanks to our BIMA coordinators Joanna, Raili, and the entire BIMA department too, who helped me directly and indirectly in my whole study period.

Finally, I would also like to thank my parents and my wife, Mandila Shrestha, whose continuous support has brought me to complete this study.

9. References

Alexander-Bryant, A.A., W.S.V. Berg-Foels, and X., Wen. 2013. Bioengineering Strategies for Designing Targeted Cancer Therapies. *Advances in Cancer Research*. 118:1–59.

Andrade, E.M., P. Ali , A.M.A. Gallegos, and G.A. Favela. 2017. Microfluidics technology for drug delivery A review. *Frontiers in Bioscience*. 10:400–414.

Azonano, 2006. Quantum Dots – A Definition, How They Work, Manufacturing, Applications and Their Use In Fighting Cancer. *AZoNano.com*.

Bachelder, E.M., E.N. Pino, and K.M. Ainslie. 2016. Acetalated Dextran: A Tunable and Acid-Labile Biopolymer with Facile Synthesis and a Range of Applications. *Chemical Reviews*. 117:1915–1926.

Bharti, C., N. Gulati, U. Nagaich, and A.K. Pal. 2015. Mesoporous silica nanoparticles in target drug delivery system: A review. *International Journal of Pharmaceutical Investigation*. 5:124.

Buzea, C., I.I. Pacheco, and K. Robbie. 2007. Nanomaterials and nanoparticles: Sources and toxicity. *Biointerphases*. 2.

Cai, W. and Chen, F. 2017. *Hybrid Nanomaterials: Design, Synthesis, and Biomedical Applications*. 1st ed. Taylor & Franccis, NY: CRC Press.

Cao, Y., Y. Gong, L. Liu, Y. Zhou, X. Fang, C. Zhang, Y. Li, and J. Li. 2017. The use of human umbilical vein endothelial cells (HUVECs) as an *in vitro* model to assess the toxicity of nanoparticles to endothelium: a review. *Journal of Applied Toxicology*. 37:1359–1369.

Carvalho, A., A.R. Fernandes, and P.V. Baptista. 2019. Nanoparticles as Delivery Systems in Cancer Therapy. *Applications of Targeted Nano Drugs and Delivery Systems*. 257–295.

Castillo, RR. and Vallet-Regí, M. 2019. Functional Mesoporous Silica Nanocomposites: Biomedical applications and Biosafety. *International Journal of Molecular Sciences*. 20(4).

Cha, C., S.R. Shin, N. Annabi, M.R. Dokmeci, and A. Khademhosseini. 2013. Carbon-Based Nanomaterials: Multifunctional Materials for Biomedical Engineering. *ACS Nano*. 7:2891–2897.

Chen, F., H. Hong, S. Goel, S.A. Graves, H. Orbay, E.B. Ehlerding, S. Shi, C.P. Theuer, R.J. Nickles, and W. Cai. 2015. *In Vivo* Tumor Vasculature Targeting of CuS@MSN Based Theranostic Nanomedicine. *ACS Nano*. 9:3926–3934.

Chen, F., Hong, H., Goel, S., Valdovinos, H., Nickles, R., and Cai, W. 2014. A multifunctional CuS@MSN nanoplatform for tumor targeted PET imaging, drug delivery, and photothermal therapy. *J Nucl Med.* 55(168).

Cohen, J.L., S. Schubert, P.R. Wich, L. Cui, J.A. Cohen, J.L. Mynar, and Fréchet Jean M. 2011. Acid-Degradable Cationic Dextran Particles for the Delivery of siRNA Therapeutics. *Bioconjugate Chemistry*. 22:1056–1065.

Damiati, S., U. Kompella, S. Damiati, and R. Kodzius. 2018. Microfluidic Devices for Drug Delivery Systems and Drug Screening. *Genes*. 9:103.

Doan, T.L.H., Mai, N.X.D., Matsumoto, K. and Tamanoi, F. 2018. Tumor Targeting and Tumor Growth Inhibition Capability of Mesoporous Silica Nanoparticles in Mouse Models. *The Enzymes*. 44:61-68.

Douroumis, D., Onyesom, I., Maniruzzaman, M. and Mitchell, J. 2012. Mesoporous silica nanoparticles in nanotechnology. *Critical Reviews in Biotechnology*. 33(3):229-245.

DrugBank. 2020. Methylprednisolone. *DrugBank*.

DrugBank. 2020. Tacrolimus *DrugBank*.

Ec.europa.eu. 2020. Nanotechnologies. *Europa.Eu.*

Enrico, C. 2018. Nanotheranostics and theranostic nanomedicine for diseases and cancer treatment. *Design of Nanostructures for Theranostics Applications*. 41–68.

Fellers, T.J., and M.W. Davidson. 2020. Introduction to Confocal Microscopy. Olympus. USA

Fröhlich, E. 2012. The role of surface charge in cellular uptake and cytotoxicity of medical nanoparticles. *International Journal of Nanomedicine*. 5577.

G BioSciences. 2013. *CytoScan™ WST-1 Cell Cytotoxicity Assay*. A Geno Technology, Inc. USA
Gray, R., and P. Abdulkin. 2018. MICROFLUIDICS - Taking a Microfluidics Approach to Drug Delivery. *Drug Development and Delivery*.

Gujrati, M., Malamas, A., Shin, t., Jin, E., Sun, Y. and Lu, Z-R. 2014. Multifunctional cationic lipid-based nanoparticles facilitate endosomal escape and reduction-triggered cytosolic siRNA release. *Mol. Pharm.* 11 (8):2734-2744.

Harun, S.N., H. Ahmad, H.N. Lim, S.L. Chia, and M.R. Gill. 2021. Synthesis and Optimization of Mesoporous Silica Nanoparticles for Ruthenium Polypyridyl Drug Delivery. *Pharmaceutics*. 13:150.

He, Y., L. Luo, S. Liang, M. Long, and H. Xu. 2017. Amino-functionalized mesoporous silica nanoparticles as efficient carriers for anticancer drug delivery. *Journal of Biomaterials Applications*. 32:524–532.

Hu, Y., L. Ke, H. Chen, M. Zhuo, X. Yang, D. Zhao, S. Zeng, and X. Xiao. 2017. Natural material-decorated mesoporous silica nanoparticle container for multifunctional membrane-controlled targeted drug delivery. *International Journal of Nanomedicine*. Volume 12:8411–8426.

Ibdi, 2020. Confocal Microscopy. Microscopy Techniques and Culture Surfaces: Find the Perfect Match. *Ibidi*.

Iso.org. 2020. Nanotechnologies — Vocabulary — Part 1: Core terms. *Online Browsing Platform (OBP*), ISO.

Jeevanandam, J., A. Barhoum, Y.S. Chan, A. Dufresne, and M.K. Danquah. 2018. Review on nanoparticles and nanostructured materials: history, sources, toxicity and regulations. *Beilstein Journal of Nanotechnology*. 9:1050–1074.

Joseph, E., and G. Singhvi. 2019. Multifunctional nanocrystals for cancer therapy: a potential nanocarrier. *Nanomaterials for Drug Delivery and Therapy*. 91–116.

Kalash, R.S., V.K. Lakshmanan, C.-S. Cho, and I.-K. Park. 2016. Theranostics. *Biomaterials Nanoarchitectonics*. 197–215.

Karimi, M., H. Mirshekari, M. Aliakbari, P. Sahandi-Zangabad, and M.R. Hamblin. 2016. Smart mesoporous silica nanoparticles for controlled-release drug delivery. *Nanotechnology Reviews*. 5.
Khan, I., Saeed, K. and Khan, I. 2019. Nanoparticles: Properties, applications and toxicities. *Arabian Journal of Chemistry*. 12 (7):908-931.

Khan, S., M. Shaharyar, M. Fazil, M.Q. Hassan, S. Baboota, and J. Ali. 2016. Tacrolimus-loaded nanostructured lipid carriers for oral delivery-*in vivo* bioavailability enhancement. *European Journal of Pharmaceutics and Biopharmaceutics*. 109:149–157.

Kim, M.-K., D.-H. Ki, Y.-G. Na, H.-S. Lee, J.-S. Baek, J.-Y. Lee, H.-K. Lee, and C.-W. Cho. 2021. Optimization of Mesoporous Silica Nanoparticles through Statistical Design of Experiment and the Application for the Anticancer Drug. *Pharmaceutics*. 13:184.

Kocherova, I., A. Bryja, P. Mozdziak, A. Angelova Volponi, M. Dyszkiewicz-Konwińska, H. Piotrowska-Kempisty, P. Antosik, D. Bukowska, M. Bruska, D. Iżycki, M. Zabel, M. Nowicki, and B. Kempisty. 2019. Human Umbilical Vein Endothelial Cells (HUVECs) Co-Culture with Osteogenic Cells: From Molecular Communication to Engineering Prevascularised Bone Grafts. *Journal of Clinical Medicine*. 8:1602.

Lalwani, G. and B. Sitharaman. 2013, Multifunctional fullerene- and Metallofullerene- based nanobiomaterials. *Nano Life*. 03:1342003.

Lamprecht, A., H. Yamamoto, H. Takeuchi, and Y. Kawashima. 2005. A pH-sensitive microsphere system for the colon delivery of tacrolimus containing nanoparticles. *Journal of Controlled Release*. 104:337–346.

Li, Y., M. Cupo, L. Guo, J. Scott, B. Yan, and W. Lu. 2015. *Cancer Photothermal Chemo Therapy Using Hollow Copper Sulfide Doxorubicin Nanoparticles*. The University of Rhode Island, United States.

Li, Y., Scott, J. and Lu, W. 2015. *Facile Direct Dry Grinding Synthesis of Monodisperse Lipophilic CuS Nanoparticles*. The University of Rhode Island, United States.

Li, Y., Yan, B. and Lu, W. 2015. *Cancer Photothermal Therapy and CuS Nanoparticles*. The University of Rhode Island, United States.

Li, Z., Barnes, JC., Bosoy, A., Stoddart JF and Zink JI. 2012. Mesoporous silica nanoparticles in biomedical applications. *Chem Soc Rev*. 41(7):2590-605.

Lifeline Cell Tech Team. 2020. 'Why Use HUVEC Cells?'. *Lifeline Cell Technology.*

Lim, J.K., S.P. Yeap, H.X. Che, and S.C. Low. 2013. Characterization of magnetic nanoparticle by dynamic light scattering. *Nanoscale Research Letters*. 8.

Lin, S., C. Ge, D. Wang, Q. Xie, B. Wu, J. Wang, K. Nan, Q. Zheng, and W. Chen. 2019. Overcoming the Anatomical and Physiological Barriers in Topical Eye Surface Medication Using a Peptide-Decorated Polymeric Micelle. *ACS Applied Materials & Interfaces*. 11:39603–39612.

Lion, N., F. Reymond, H.H. Girault, and J.S. Rossier. 2004. Why the move to microfluidics for protein analysis? *Current Opinion in Biotechnology*. 15:31–37.

Liu, H-J., and Xu, P. 2019. Smart Mesoporous Silica Nanoparticles for Protein Delivery. *Nanomaterials.* 9(4):511.

Liu, L., J. Li, M.-hui Zhao, H. Xu, L.-sen Li, and S.-ning Wang. 2016. Loading of tacrolimus containing lipid based drug delivery systems into mesoporous silica for extended release. *Asian Journal of Pharmaceutical Sciences*. 11:751–759.

LS Instruments. 2020. LS Instruments. *Dynamic Light Scattering*.

Lu, F., J. Wang, L. Yang, and J.-J. Zhu. 2015. A facile one-pot synthesis of colloidal stable, monodisperse, highly PEGylated CuS@mSiO2 nanocomposites for the combination of photothermal therapy and chemotherapy. *Chemical Communications*. 51:9447–9450.

Lu, F., W. Qian, C. Zhan, Q. Wang, Q. Shen, J. Zhong, Q. Fan, and W. Huang. 2019. Facile synthesis of hollow mesoporous silica nanoparticles with in-situ formed CuS templates. *Materials Letters*. 250:25–29.

Lu, G.W., and P. Gao. 2010. Emulsions and Microemulsions for Topical and Transdermal Drug Delivery. *Handbook of Non-Invasive Drug Delivery Systems*. 59–94.

Lu, L. 2018. *Droplet Microfluidics: T-Junction - Lina Wu*. Openwetware.

Luo, G., L. Du, Y. Wang, and K. Wang. 2015. Composite Nanoparticles. *Encyclopedia of Microfluidics and Nanofluidics*. 453–460.

Luo, G.-F., W.-H. Chen, Y. Liu, Q. Lei, R.-X. Zhuo, and X.-Z. Zhang. 2014. Multifunctional Enveloped Mesoporous Silica Nanoparticles for Subcellular Co-delivery of Drug and Therapeutic Peptide. *Scientific Reports*. 4.

Malm, A.V., and J.C. Corbett. 2019. Improved Dynamic Light Scattering using an adaptive and statistically driven time resolved treatment of correlation data. *Scientific Reports*. 9.

Mansha, M., Qurashi, A., Ullah, N., Bakare, F.O., Khan, I. and Yamani, Z.H. 2016. Synthesis of In2O3/graphene heterostructure and their hydrogen gas sensing properties. *Ceramics International*. 42 (9):11490-11495.

Mashaghi, S., A. Abbaspourrad, D.A. Weitz, and A.M. van Oijen. 2016. Droplet microfluidics: A tool for biology, chemistry and nanotechnology. *TrAC Trends in Analytical Chemistry*. 82:118–125.

Mayo Clinic (2020). End-stage renal disease. *Mayo Foundation for Medical Education and Research*
Mendes, M., J. Sousa, A. Pais, and C. Vitorino. 2018. Clinical applications of nanostructured drug delivery systems: From basic research to translational medicine. *Core-Shell Nanostructures for Drug Delivery and Theranostics*. 43–116.

Merck. 2020. *DAPI for nucleic acid staining*. Sigma-Aldrich, Inc.

Merck. 2020. *Protocol Guide: WST-1 Assay for Cell Proliferation and Viability*. Sigma-Aldrich, Inc.

Mousavi, S.S.A., S.T. Wereley, and N.-T. Nguyen. 2019. Fundamentals and Applications of Microfluidics. Third. Artech House, Norwood, MA.

Nano.gov. 2021. What Is Nanotechnology?. *Nano.gov*.

Ngamcherdtrakul, W., T. Sangvanich, M. Reda, S. Gu, D. Bejan, and W. Yantasee. 2018. Lyophilization and stability of antibody-conjugated mesoporous silica nanoparticle with cationic polymer and PEG for siRNA delivery. *International Journal of Nanomedicine*. Volume 13:4015–4027.

Ngan, V. 2004. Tacrolimus. *Tacrolimus | DermNet NZ*. DermNet New Zealand Trust.

Pacific Biolabs. 2020. Cell Based Assays. *Pacific Biolabs*.

Paiva, M.R., G.F. Andrade, L.F. Dourado, B.F. Castro, S.L. Fialho, E.M. Sousa, and A. Silva-Cunha. 2020. Surface functionalized mesoporous silica nanoparticles for intravitreal application of tacrolimus. *Journal of Biomaterials Applications*. 35:1019–1033.

Park, S., H. Park, S. Jeong, B.G. Yi, K. Park, and J. Key. 2019. Hyaluronic Acid-Conjugated Mesoporous Silica Nanoparticles Loaded with Dual Anticancer Agents for Chemophotodynamic Cancer Therapy. *Journal of Nanomaterials*. 2019:1–11.

Peng, S., and H. Chen. 2018. Biocompatible CuS-based nanoplatforms for efficient photothermal therapy and chemotherapy *in vivo*
. *Nanomedicine: Nanotechnology, Biology and Medicine*. 14:1843.

Perez, X.E.B. 2019. Nanoparticle Synthesis for Glucose-Loaded Mesoporous Silica and Sucrose Hydrolysis Strategies for Bioanalyte Detection Applications using a Personal Glucose Meter. E Graduate School at Scholar Commons.

Pubchem. 2005. Tacrolimus. *National Center for Biotechnology Information. PubChem Compound Database*. Tacrolimus | C44H69NO12 - PubChem (nih.gov)

Puri, A., Loomis, K., Smith, B., Lee, J.H., Yavlovich, A., Heldman, E. and Blumenthal, R. 2009. Lipid-based nanoparticles as pharmaceutical drug carriers: from concepts to clinic. *Crit. Rev. Ther. Drug Carrier Syst*. 26 (6):523-580.

Robertson, J., Rizzello, L., Avila-Olias, M., Gaitzsch, J., Contini, C., Magoń, M., Renshaw, S. and Battaglia, G., 2016. Purification of Nanoparticles by Size and Shape. *Scientific Reports*, 6(1).

Rouquerol, J., D. Avnir, C.W. Fairbridge, D.H. Everett, J.M. Haynes, N. Pernicone, J.D. Ramsay, K.S. Sing, and K.K. Unger. 1994. Recommendations for the characterization of porous solids (Technical Report). *Pure and Applied Chemistry*. 66:1739–1758.

RxList. 2018. Medrol *RxList*.

RxList. 2018. PROGRAF. *RxList*.

ScienceDaily, 2020. Nanoparticle. *ScienceDaily*.

Sigmund, W., Yuh, J., Park, H., Maneeratana, V., Pyrgiotakis, G., Daga, A., Taylor, J. and Nino, J.C. 2006. Processing and structure relationships in electrospinning of ceramic fiber systems. *Journal of American Ceramic* Society. 89 (2):395-407.

Stroock, A.D. 2008. MICROFLUIDICS. *Optical Biosensors*. 659–681.

Sudha, P.N., K. Sangeetha, K. Vijayalakshmi, and A. Barhoum. 2018. Nanomaterials history, classification, unique properties, production and market. *Emerging Applications of Nanoparticles and Architecture Nanostructures*. 341–384.

Sun, J.-G., Q. Jiang, X.-P. Zhang, K. Shan, B.-H. Liu, C. Zhao, and B. Yan. 2019. Mesoporous silica nanoparticles as a delivery system for improving antiangiogenic therapy. *International Journal of Nanomedicine*. Volume 14:1489–1501.

Sun, S., Murray, C.B., Weller, D., Folks, L. and Moser, A. 2000. Monodisperse FePt nanoparticles and ferromagnetic FePt nanocrystal superlattices. *Science*. 287:1989-1992.

Taylor, D.A. 2002. Dust in the Wind. *Environmental Health Perspectives*. 110:A80–A87.

Thomas, D.L. 2019. Benefits of Using a Microfluidic Device. *News*.

Thomas, S., Harshita, B.S.P., Mishra, P. and Talegaonkar, S. 2015. Ceramic nanoparticles: fabrication methods and applications in drug delivery. *Current Pharmaceutical Design*. 21 (45):6165-6188.
Tomeh, M.A., and X. Zhao. 2020. Recent Advances in Microfluidics for the Preparation of Drug and Gene Delivery Systems. *Molecular Pharmaceutics*. 17:4421–4434.

Tsuneo, T., Toshio, S., Kazuyuki, K. and Chuzo, K. 1990. 1 The Preparation of Alkyltriinethylaininonium–Kaneinite Complexes and Their Conversion to Microporous Materials. 1990. *CSJ Journals*. 63 (4):988-992.
Ushikubo, F.Y., F.S. Birribilli, D.R. Oliveira, and R.L. Cunha. 2014. Y- and T-junction microfluidic devices: effect of fluids and interface properties and operating conditions. *Microfluidics and Nanofluidics*. 17:711–720.

Valenti, G., Rampazzo, E., Bonacchi, S., Petrizza, L., Marcaccio, M., Montalti, M., Prodi, L., and Paolucci, F. 2016. Variable Doping Induces Mechanism Swapping in Electrogenerated Chemiluminescence of Ru(bpy)32+ Core–Shell Silica Nanoparticles. *Journal of the American Chemical Society*. 138(49):15935-15942.

Vallet-Regi, M., Rámila, A., Real, R. P. del. and Pérez-Pariente, J. 2001. A New Property of MCM-41: Drug Delivery System. *Chemistry of materials*. 13(2):308-311.

Vazquez, N.I., Z. Gonzalez, B. Ferrari, and Y. Castro. 2017. Synthesis of mesoporous silica nanoparticles by sol–gel as nanocontainer for future drug delivery applications. *Boletín de la Sociedad Española de Cerámica y Vidrio*. 56:139–145.

Virlan, M., D. Miricescu, R. Radulescu, C. Sabliov, A. Totan, B. Calenic, and M. Greabu. 2016. Organic Nanomaterials and Their Applications in the Treatment of Oral Diseases. *Molecules*. 21:207.
Wang, S., F. Fontana, M.-A. Shahbazi, and H.A. Santos. 2021. Acetalated dextran based nano- and microparticles: synthesis, fabrication, and therapeutic applications. *Chemical Communications*. 57:4212–4229.

Williams, D.B., and C.B. Carter. 1996. Imaging in the TEM. *Transmission Electron Microscopy*. 349–366.
Wu, L., M. Wu, Y. Zeng, D. Zhang, A. Zheng, X. Liu, and J. Liu. 2014. Multifunctional PEG modified DOX loaded mesoporous silica nanoparticle@CuS nanohybrids as photo-thermal agent and thermal-triggered drug release vehicle for hepatocellular carcinoma treatment. *Nanotechnology*. 26:025102.

Wu, S.-H., C.-Y. Mou, and H.-P. Lin. 2013. Synthesis of mesoporous silica nanoparticles. *Chemical Society Reviews*. 42:3862.

Yang, J., D. Dai, X. Lou, L. Ma, B. Wang, and Y.-W. Yang. 2020. Supramolecular nanomaterials based on hollow mesoporous drug carriers and macrocycle-capped CuS nanogates for synergistic chemo-photothermal therapy. *Theranostics*. 10:615–629.

Zengin, A., P. Sutthavas, and S. van Rijt. 2020. Inorganic nanoparticle-based biomaterials for regenerative medicine. *Nanostructured Biomaterials for Regenerative Medicine*. 293–312.

Zhang, L., Q. Chen, Y. Ma, and J. Sun. 2019. Microfluidic Methods for Fabrication and Engineering of Nanoparticle Drug Delivery Systems. *ACS Applied Bio Materials*. 3:107–120.

Zhang, L., Y. Li, Z. Jin, J.C. Yu, and K.M. Chan. 2015. An NIR-triggered and thermally responsive drug delivery platform through DNA/copper sulfide gates. *Nanoscale*. 7:12614–12624.

Zhang, Y., M. Xiong, X. Ni, J. Wang, H. Rong, Y. Su, S. Yu, I.S. Mohammad, S.S. Leung, and H. Hu. 2021. Virus-Mimicking Mesoporous Silica Nanoparticles with an Electrically Neutral and Hydrophilic Surface to Improve the Oral Absorption of Insulin by Breaking Through Dual Barriers of the Mucus Layer and the Intestinal Epithelium. *ACS Applied Materials & Interfaces*.

Zhao, T., Nguyen, N-T., Xie, Y., Sun, X., Li, Q., and Li, X. 2017. Inorganic Nanocrystals Functionalized Mesoporous Silica Nanoparticles: Fabrication and Enhanced Bio-applications. *Frontier of Chemistry.* 5